EX VIVO GENERATION OF DENDRITIC CELLS WITHIN A VASCULAR BIOREACTOR

By

PATRICK WILLIAMSON

Bachelor of Science in Chemical Engineering

Oklahoma State University

Stillwater, OK

2017

Submitted to the Faculty of the
Graduate College of the
Oklahoma State University
in partial fulfillment of
the requirements for
the Degree of
MASTER OF SCIENCE
May, 2019

EX VIVO GENERATION OF DENDRITIC CELLS

WITHIN A VASCULAR BIOREACTOR

Thesis Approved:

Dr. Heather Fahlenkamp

Thesis Adviser

Dr. Yu Feng

Dr. Josh Ramsey

ACKNOWLEDGEMENTS

I want to thank Dr. Lin Liu at Center for Veterinary Health Sciences at Oklahoma State University for allowing us to use his flow cytometer. I would also like to thank Dr. Meinkoth at the Center for Veterinary Health Sciences for his help with Wright-Giesma staining. I also want to thank Larry Vaughn of OSU's Physics and Chemistry instrument shop for helping in the fabrication of the bioreactor. This project was funded by a grant from the Oklahoma Center for the Advancement of Science and Technology (HR16-144).

Name: PATRICK WILLIAMSON

Date of Degree: May, 2019

Title of Study: EX VIVO GENERATION OF DENDRITIC CELLS WITHIN A VASCULAR BIOREACTOR

Major Field: CHEMICAL ENGINEERING

Abstract: Dendritic cells (DCs) play a prime role in the activation and control of the immune system and have promising potential in the treatment of cancer, viral infection, autoimmune diseases and transplantation rejection. DCs can be generated ex vivo from human monocytes by the use of growth factors or during transendothelial migration. Many studies have generated DCs under static, "no flow" conditions. However, such studies do not mimic the "flow" occurring in the capillaries. The objective of this study was to see if we could generate functional DCs within a novel bioreactor system under flow conditions. A HUVEC monolayer was grown on a porous membrane and added it to a bioreactor at 0.4 mL/min. Inflammation was mimicked by adding TNF-α to the system for 48 h. Cell morphology, viability, CAM expression and MCP-1 were measured. CFSE-labeled monocytes were added above the flow path. Monocytes were analyzed for location based on fluorescent intensity and migration markers. Finally, we looked at the differentiation of monocytes into DCs by looking at common DC markers. To test for functionality, we performed a mixed leukocyte reaction (MLR) for seven days and measured proliferation and activation of T-cells.

HUVECs maintained a compact network after 72 h. Cell viability with and without TNF-α was 78% and 82%, respectively. Increased VCAM-1 expression (37%) and MCP-1 (6x) act as inflammatory responses to send signals for recruitment of leukocytes. Increased monocyte migration through the stimulated endothelium could be due loose HUVEC junctions. All migration marker expression was downregulated in a stimulated system, possibly due to monocyte shifting away from lineage or differentiation into DCs. DCs from the bioreactor had no morphological differences when compared to static culture. DCs attached to the endothelium expressed 80% CD206, possibly playing a role in their attachment to the endothelium. DCs after culture expressed CD86 and after adding maturation cytokines, bioreactor and static DCs matured as indicated by CD83 expression (72% and 84.9%, respectively). DCs from the bioreactor proliferated activated T-cells more than static DCs as indicated by MFI. Overall, the system was able to generate functional DCs that promoted better T-cell proliferation than traditional methods.

Table of Contents

Chapter **Page**

LIST OF FIGURES

LIST OF TABLES

Chapter I

Introduction

The immune system is the body's defense mechanism against viral infections, diseases and foreign pathogens. It can play a key role in curing cancer, transplantation rejection, and autoimmune diseases by identifying and eliminating pathogens while distinguishing healthy cells from one's own body. Dendritic cells (DCs) are one of the key components of the innate immune response. Howard et al describe DCs as the one control point of the immune system [1]. DCs are initiators and modulators of the immune response by efficiently stimulating T and B cells [2]. Just how important are DCs for T-cells during an immune response? T-cells have to be able recognize peptides located on infected cells at frequencies of 1/100,000 or less [2]. DCs, located in majority of tissues, can capture and process antigens which will then be displayed on their surface in large quantities. These mobile cells can then migrate into tissue and present the specific antigen to T-cells, thus activating and beginning the defense mechanism. DCs are able to stimulate proliferation of T-cells almost 100x more than macrophages or other lymphoid subpopulations [3].

DC population within blood is relatively low, with the percentage of total cells around 1-2%. Currently in research settings, DCs are typically generated in static cultures from monocytes by the use of cytokines and growth factors, such as granular-macrophage colony-stimulating factor (GM-CSF) and interleukin (IL)-4, as first discovered by Sallusto and Lanzavecchia [4]. They

were able to generate immature DCs, which are better at capturing soluble antigens. After addition of tumor necrosis factor (TNF)-α, DCs generated using this method have a better ability to present and stimulate allogenic T-cells than previous $CD34^+$ precursor cells. Randolph et al showed also that monocytes could differentiate into DCs after migration across an endothelium layer without the presence of additional cytokines [5]. They also showed DCs predominantly reverse transmigrated, while macrophages did not. Endothelial cells (ECs) line every blood vessel and are important for tissue growth and repair. The ability to migrate back and forth across a tissue layer is another important feature of DCs. Shukla followed up on this and showed that the number of monocytes that differentiated into immature DCs across an EC layer increased as glucose concentration increased on a 3D collagen matrix tissue model [6].

Although good representations of cell behavior in response to certain variations, these 3D vascular constructs studied previously still lack many physiological effects taking place *in vivo* [5, 6]. Bioreactors have emerged as a way to combine the dynamic effects similar to *in vivo* conditions with traditional static cell cultures. Bioreactors have been shown to increase cell viability, function and cell alignment more resemblant of how they are in the body [7, 8]. DCs have been generated in a dynamic system but they failed to show significant increase in functionality when compared to static DCs due possibly to it being microgravity system [9]. Previous works with vascular constructs were done in batch systems, by putting cells in and removing all at once after culture. Although effective, this process leads to cell loss and longer times in between experiments. A continuous process could reduce both of those and generate more cells at the same time. To the best of our knowledge, there have been no studies that have added monocytes above the flow path of a vascular tissue construct in order to generate DCs ex vivo. This method leads to cells migrating beneath the vascular construct while still having the

ability to add more precursor cells above simultaneously. Because of this, we propose a new system that hopefully is able to generate functional DCs similar to those grown in traditional static cultures.

Problem Statement

The overall goal is to develop a novel continuous system that can produce functional DCs by constructing a tissue-engineered construct within a bioreactor. The design will be based on previous works that will be co-culturing endothelial cells with monocytes except along with studying the migration, we will also look to analyze the functionality of DCs generated from monocytes [5, 6]. The long-term goal is to be able to develop a patient specific DC-based therapeutic that could be used to treat a variety of diseases. This research is the initial step toward obtaining that goal. The hypothesis is that DCs generated in a novel vascular construct will be better stimulators for proliferation of T-cells than traditional methods. This research was done in three parts to establish a system for generation of DCs.

a. Characterize the 3D vascular tissue construct within a bioreactor with flow conditions.

The first objective was to characterize a vascular tissue construct after introducing it to a bioreactor under flow conditions. After 72 h, we analyzed cell morphology using fluorescent microscopy. We measured cell viability and common cellular adhesion molecules (CAMs) by using of flow cytometry. We also looked at release of a soluble protein related to recruitment of monocytes. An inflammatory stimulus was added for some studies to investigate the effects on the vascular tissue construct.

b. Characterize monocyte migration within the bioreactor.

For this aim, we characterized monocyte migration within various regions in the bioreactor. After the vascular tissue construct had been added for 24 h with and without an inflammatory stimulus, monocytes labeled with a fluorescent probe were added to the system for the final 48 h. Monocyte location was measured by fluorescent intensity using a standard curve. Monocytes were also analyzed by flow cytometry for surface protein expression related to migration.

c. Characterize DCs generated in a bioreactor system

DCs have been studied extensively on their role in immune response and how different generation techniques affect their functionality. Most studies generate DCs from monocytes by using certain growth factors, such as granulocyte-macrophage colony-stimulating factor (GM-CSF) and IL-4 in 2D culture system. Here, we added monocytes to the bioreactor with a vascular construct and studied their differentiation into DCs without additional cytokines. In order to test for DCs differentiated in the bioreactor system, we used flow cytometry to analyze key DC surface markers. Once generated, cells were tested for functionality using a mixed leukocyte reaction (MLR) with autologous T-cells. We compared how loading DCs with an antigen affected their ability to stimulate proliferation and activation of T-cells.

Chapter II

Background

2.1 Inflammatory Response

The human body is constantly fighting millions of toxic and pathogenic microbes that enter its systems daily. The defense mechanism utilized to combat foreign and dangerous microbes is the immune system. Failure to eliminate any inflammation can cause severe tissue damage. An immune response happens in four common steps: surface receptors detect foreign stimuli; inflammatory pathways are activated; inflammatory stimuli are released; and inflammatory response cells are recruited. Toll-like receptors on macrophages detect when a foreign pathogen is present and release inflammatory chemokines and cytokines such as tumor-necrosis factor (TNF)-α and interleukin (IL)-6 to indicate where localization of neutrophils and monocytes should be [10, 11]. Inflammatory response cells then work together to eliminate the pathogen, with monocytes differentiating into DCs and macrophages; macrophages undergoing phagocytosis; DCs stimulating T-cell and B-cell response and mast cells releasing inflammatory mediators. When cells are not able to limit or suppress the inflammation, inflammation is then considered to be chronic. This could be due to a number of factors like chronic infections, failing to regulate T-cell response, and autoimmune cells attacking healthy host cells [10, 11]. Resolution of inflammation begins when pro-resolving mediators such as nuclear factor kappa B

(NF-κB) are turned on. Expression of NF-κB results in downregulation of TNF-α, decreasing the recruitment of neutrophils and other leukocytes to the site of inflammation [12]. Neutrophils at the site of inflammation begin to undergo apoptosis and are cleared by macrophages, therefore returning the tissue to homeostasis.

2.2 Blood vessels

The ECs are the so called "gate keepers", regulating cell, nutrient, and waste passage to and from the blood. Complications with growth or maintenance can lead to a stroke, inflammatory disorders, blinding eye disease and pulmonary hypertension [13]. White blood cells continually will circulate in the blood, looking for any infection or damage done in the body. Once an abnormality is discovered, vascular cells release cytokines to recruit various leukocytes to that location. These cytokines can then alter cells receptors or adhesion molecules of ECs lining the blood vessels which in turn affect leukocytes ability to attach, roll and then transmigrate through endothelium junctions. The vascular endothelium can also express lymphocyte costimulatory molecules which can stimulate proliferation of T-cells [14].

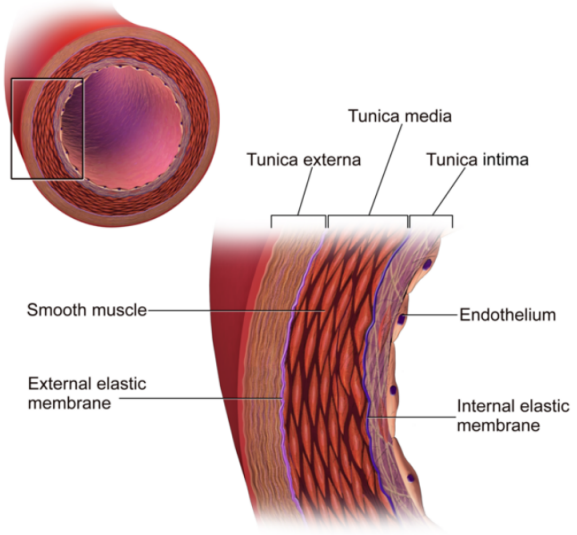

Figure 1. Structure of blood vessel. Taken from https://courses.lumenlearning.com/boundless-ap/chapter/blood-vessel-structure-and-function/

2.3 Cells

2.3.1 Endothelial Cells

In an adult human, ECs account for approximately 6 x 10^{13} cells and cover up to 7 m^2 of surface area [15]. In research, ECs have been used to study inflammation, atherosclerosis, diabetes, and study the effect of pharmaceuticals and their ability to penetrate the blood-tissue barrier[16]. When ECs are under normal conditions, they do not interact with leukocytes due to suppressing interactive proteins such as P-selectin and chemokines [17, 18]. During an acute inflammation, ECs have two types of activation methods. Type I activation consist mainly of elevated release of Ca^{2+} from endoplasmic reticulum storage [18]. Release of more Ca^{2+} leads activation of the myosin-light-chain kinase (MLCK), producing myosin light chain (MLC) which cause ECs to begin contracting to open up junctions between adjacent ECs [19]. The loose EC membranes allow for leukocytes to pass through the endothelium by the interaction of CD31 (PECAM-1)

and CD99 on ECs, which are important for transmigration [20]. Type II activation occurs when the inflammation is more damaging. Tumor-necrosis factor (TNF)-α is released from activated leukocytes and binds to domains of TNF receptor 1 on ECs [18, 21]. This activation then leads to looser junctions and increased leukocyte recruitment to activation site. Increased amounts of TNF-α bound to ECs has also shown to increase the expression of CD54 (ICAM-1) and CD106 (VCAM-1) as well as an increase in secretion of monocyte chemoattractant protein (MCP-1) and IL-8 [16, 18]. TNF-α has also been shown to trigger cell death after exposure for a lengthy period of time [18].

2.3.2 Monocytes

Monocytes are one of the most pivotal cells part of the immune system. They play a major role in defending the body against infectious diseases and can differentiate into macrophages or DCs [22]. Monocytes are characterized by their bean shape nuclei and expression of CD11b, CD11c and CD14 [23]. Monocytes account for approximately 10% of leukocytes in blood originating out of bone marrow [24]. From there, monocytes migrate into the blood where they patrol the vascular system and eventually migrate into tissues such as spleen, liver and lungs. In humans, monocytes are characterized by three subsets of their phenotypic expression: $CD14^{+}CD16^{-}$ (classical), $CD14^{+}CD16^{+}$(intermediate), $CD14^{dim}CD16^{+}$ (non-classical) [24]. Classical monocytes are $CCR2^{+}$, produce high levels of IL-10 and respond to toll-like receptors (TLR) 2 and 4 ligands while non-classical monocytes lack CCR2 and respond to viral stimuli [25, 26]. Classical monocytes major role phagocytosis and express genes involved in angiogenesis, wound healing and coagulation [26].

When an inflammation occurs, monocytes undergo a change to either DCs or macrophages depending on cytokines and transcription factors present. For *in vitro* studies, culturing

monocytes in GM-CSF and IL-4 cause monocytes to favor differentiation into DCs [27]. For macrophages, culturing monocytes in M-CSF or IL-32 has sufficed to generate macrophages over DCs [28].

2.3.3 Dendritic Cells

DCs are one of the most potent immune response cells part of the immune response. They have been known to play a role in many diseases such as asthma, cancer, atherosclerosis and diabetes [11]. DCs are considered the best antigen presenting cell (APC) able to stimulate T-cells [1]. DCs originate from myeloid or lymphoid progenitors and can be found in a multitude of locations throughout the body such as blood, lungs, liver, spleen, and intestine [29, 30]. Under light microscope, DCs are similar to monocytes in morphology with the exception that they have thin, long dendrites. From here, DCs are classified in many different ways based on their expression of surface molecules. Migratory conventional DCs develop out of peripheral tissues and either express CD11b or CD103 [31]. Lymphoid conventional DCs express CD4 and CD8α and play a role in priming cytotoxic $CD8^+$ T-cell responses [31]. Blood monocytes have been shown to differentiate into DCs under inflammatory conditions and can originate from all three types of monocytes. Monocyte derived DCs depend on GM-CSF *in vivo* [32]. For *in vitro* culturing of monocytes to generate DCs, GM-CSF combined with IL-4 have shown great success at generating DCs that will express CD1c and CD206 (MMR) [4, 27, 33].

Monocyte derived DCs can exist in either an immature or mature form. Having mature DCs is important as the most potent antigen presentation will occur only if they are in their maturation state. Immature DCs lead to that potent antigen presentation by capturing antigens via phagocytosis, micropinocytosis, and mediate adsorptive endocytosis via MMR receptor [2]. Antigens are processed in MHC class II compartments to be stored inside the cell. After certain

signals such as bacteria or cytokines like IL-1, GM-CSF or TNF-α, the antigens will be sent to the surface of the DC and be considered mature and activated [2]. Mature DCs will express very high levels of CD40, CD80, CD83 and CD86 and lack the CD14 marker that is found on monocytes and some immature DCs [34, 35]. With the antigen present on DC surface, T-cell receptors make contact with the DC via CD28 receptor [36]. After roughly 2 h of interaction, T-cells can begin to proliferate and upregulate their activation surface markers such as CD69 and CD25 [36, 37]. T-cells communicate back to DCs by triggering DCs with TNF-related activation cytokines which increases DC stimulatory capacity and prolongs their lifecycles [38].

2.3.3.1 2D Generation of DCs

Numerous studies have generated DCs from monocytes using cytokines [4, 33, 39]. In general, using a combination of GM-CSF and IL-4 generates immature DCs in about 7-10 days. GM-CSF has been shown to increase viability and function of DCs generated and is key to forming DCs over macrophages [40]. To fully mature DCs, the addition of TNF-α is typically added for 24-48 h. Using only TNF-α does push DCs toward maturation but mature DCs generated lack the ability to secrete IL-12 and IFN-γ, which are both involved in activation of T-cells [41]. Using a cocktail of various cytokines such as IL-1β, IL-6, PGE_2 along with TNF-α has been shown to increase the maturity and functionality of DCs generated statically [35, 41, 42].

2.3.3.2 3D Generation of DCs

By creating a 3D complex, it gives a more representative system than that of 2D. Randolph et al looked into the migration of monocytes in a 3D vascular tissue construct [5]. They found that monocytes rapidly (48 h) differentiated into DCs after exposure to an endothelium layer within their vascular tissue construct. Their work also showed that reverse migrated cells, that later were

stimulated with particles, were shown to be predominantly DCs compared to those that remained in the subendothelial matrix which were macrophages. Shukla further studied the effects of inflammation on monocyte differentiation in a vascular tissue construct [6]. He displayed that glucose acts as a proinflammatory stimulus on endothelial cells. When an inflamed endothelium was present, cells that had reverse transmigrated across the endothelium were monocyte derived immature DCs rather than other leukocytes.

2.4 Bioreactors

Bioreactors are defined as an apparatus in which biological reactions or processes are carried out. Research in cartilage, bone, vascular, skin and nervous tissue have all incorporated bioreactors to study varying effects on those cell types [43]. Outside of tissue engineering, bioreactors are used in a wide range of applications such as fermentation, waste water treatment and food processing. In cell cultures, bioreactors have been used to add a dynamic feature to culturing of cells to better mimic what is taking place *in vivo*. The reason bioreactors are so useful is because one can customize the design and control biochemical and mechanical stimuli in a controlled environment. This mechanical stimuli directs cellular activity and promotes proper morphology similar to *in vivo* [44]. Having this dynamic feature encourages cells to form their extracellular matrix in a shorter time span than if they were grown under static conditions [43]. Mechanical stimuli has also been shown to effect protein expression and cell proliferation in positive ways [45].

Another reason bioreactors are favored over static culture systems is due to them having better mass exchange of nutrients and their ability to remove cell waste while culturing. Cell size and proliferation increase within a culture requires a better mass transfer to ensure all cell layers within a system receive adequate nutrients. It has been shown in previous studies that under

static conditions, glycosaminoglycan (GAG) deposits by chondrocytes was poor after roughly 400 um from the outer surface [44]. When chondrocytes were cultured in a spinner flask bioreactor, GAG deposits were able to accumulate in the central part of the construct [44].

2.5 Current Vascular Bioreactors

2.5.1 Rotating Wall

Developed by NASA, rotating wall bioreactors (RWB) create a low-shear laminar flow, high mass transfer environment which cells free-fall as they rotate during culture. These bioreactors work by rotating the vessel horizontally with the inner chamber containing a central porous membrane and annular space submerged in medium. The medium is recirculated between the central cell culture space to the peripheral cell free space to allow for maximum mass transfer of nutrients [46]. The cells within RWB form denser tissues but are successful at sustaining viability due to a well-mixed medium that facilitated waste disposal and nutrient transfer [47]. Sanford et al. showed that ECs grown in RWB could be cultured for 30 days and form multilayer tissue like structures without any changes in morphology or function [47]. They also noticed that having ECs cultured in RWB had tighter junctions similar to brain capillaries *in vivo*. Dermenoudis and Missirlis RWB had ECs elongate and form spirals due to mechanical stimuli experienced ECs [48]. These spiral formations could be ECs gravitating toward formation of a vascular network. Unfortunately, RWB are not good representations of *in vivo* conditions.

2.5.2 Perfusion

Perfusion bioreactors offer a more similar simulation of how flow of fluid acts on cells. Fluid is pumped over the cell area either with laminar or pulsatile flow in a closed circuit loop. Geometry of the cell growth area is up to the researcher as one can change the scaffold shape dependent on need or interest. To optimize the system, researchers have computationally modeled their

perfusion bioreactor using various programs prior to experiments [49-51]. By doing this, researchers are able to better understand the actual flow the cell layer is experiencing. One key difference between perfusion and RWB is perfusion adds a pressure factor that cells will experience. Various pressure differences has been shown to effect cell attachment and proliferation [50, 51]. Many studies have shown that perfusion bioreactors routinely promote cell proliferation, uniform distribution of cells and increase in expression of key surface markers [49, 52, 53]. Perfusion bioreactors are also able to successfully provide nutrients to all cells and remove cell waste due to the constant circulation of media.

2.5.3 Parallel Plate

Parallel plate bioreactors are similar to perfusion bioreactors, where media is constantly flowing over the cell layer to create fluid shear stress except the cell layer is slightly below the flow path. Parallel plate bioreactors ideally are set up to have laminar flow over cells and the shear stress that ECs are experiencing are matched to be similar to blood vessels [54]. Parallel plate bioreactors are common for studying leukocytes through endothelium due to easiness to make and ability to observe cells during experiments. Many factors can be altered to optimize the system including channel height and volumetric flow rate. Khismatullin and Truskey noticed that the channel height effects the leukocyte adhesion, observing that having a large distance between flow path and endothelium reduces the adhesion strength even at similar *in vivo* shear stress [54]. With flow, Luscinskas et al. found that monocyte adhesion to activated ECs increased even at higher than usual shear stress [55]. Monocytes and other white blood cells were studied in a parallel plate bioreactor to see the effect of disturbed flow. Researchers found that monocytes migrated more in the reattachment area of the flow region as well as show that ICAM-1 plays a significant role in the migration of cells [56].

Chapter III

Materials and Methods

3.1 Design and Fabrication of Bioreactor

The key consideration with the bioreactor was to incorporate the addition of the vascular tissue construct. By being able to add the vascular tissue construct, cells were able to attach and reach confluency before being exposed to dynamic conditions. This design is based on previous work by Fahlenkamp and Shukla which used transwells in plates [6, 57]. The transwells were able to separate the samples into 2 chambers, with cells on a membrane used to divide the two similar to this bioreactor. The bioreactor was constructed out of Polyether Ether Ketone (PEEK) and made in-house. PEEK has an aromatic molecular backbone with ether and ketone functional groups between the aryl rings and has shown to be great for biocompatibility both *in vivo* and *in vitro* [58, 59]. Figure 2A shows a schematic of the bioreactor and Figure 2D shows the complete set-up of the bioreactor for culture. Each well (six total) has a bottom and top chamber. Six wells were chosen so that simultaneous experiments could be run in parallel. The top chamber (diameter = 15.9 mm; depth = 13.4 mm) has one inlet and exit (diameter = 2.4 mm) where media flows in and out of the well. The bottom chamber (diameter = 9.0 mm) is closed. Luer locks with barbed fittings were attached to each bioreactor well to allow for tubing connection. Tubing (1.59 cm ID, Masterflex; Gelsenkirchen, Germany) was attached to each barbed connector and

then connected to Masterflex L/S Digital drive pump (Cat. #: SI-07522-20) with multichannel pump head attached (Masterflex, Item#: HV-07534-08); thus creating a closed, recycle system. The pump was calibrated following instructions from manufacturer prior to use. A lid was placed on top of the bioreactor to help prevent contamination but allowed for gas exchange to still take place. Bioreactor, lid, fittings and tubing were autoclaved to sterilize prior to use. Pump was sterilized by UV radiation for 20 minutes prior to use. To sterilize in between experiments, 10% bleach was passed through the system for 10 min followed by 2-20 min rinses with water. After three experiments, the entire system was broken down, cleaned and autoclaved before starting another experiment.

Optimization of the flow rate was determined with the help of computational fluid dynamics (CFD). Reviewing previous literature, we wanted to select a flow rate at which cells would experience a shear force but not too much that would cause cell death or detachment from the ring. We tried 0.3, 0.4 and 0.5 mL/min flow rates. After experimenting, 0.4 mL/min showed to have the greatest viability on cells and most cell proliferation. For all experiments, 0.4 mL/min was used as the desired flow rate.

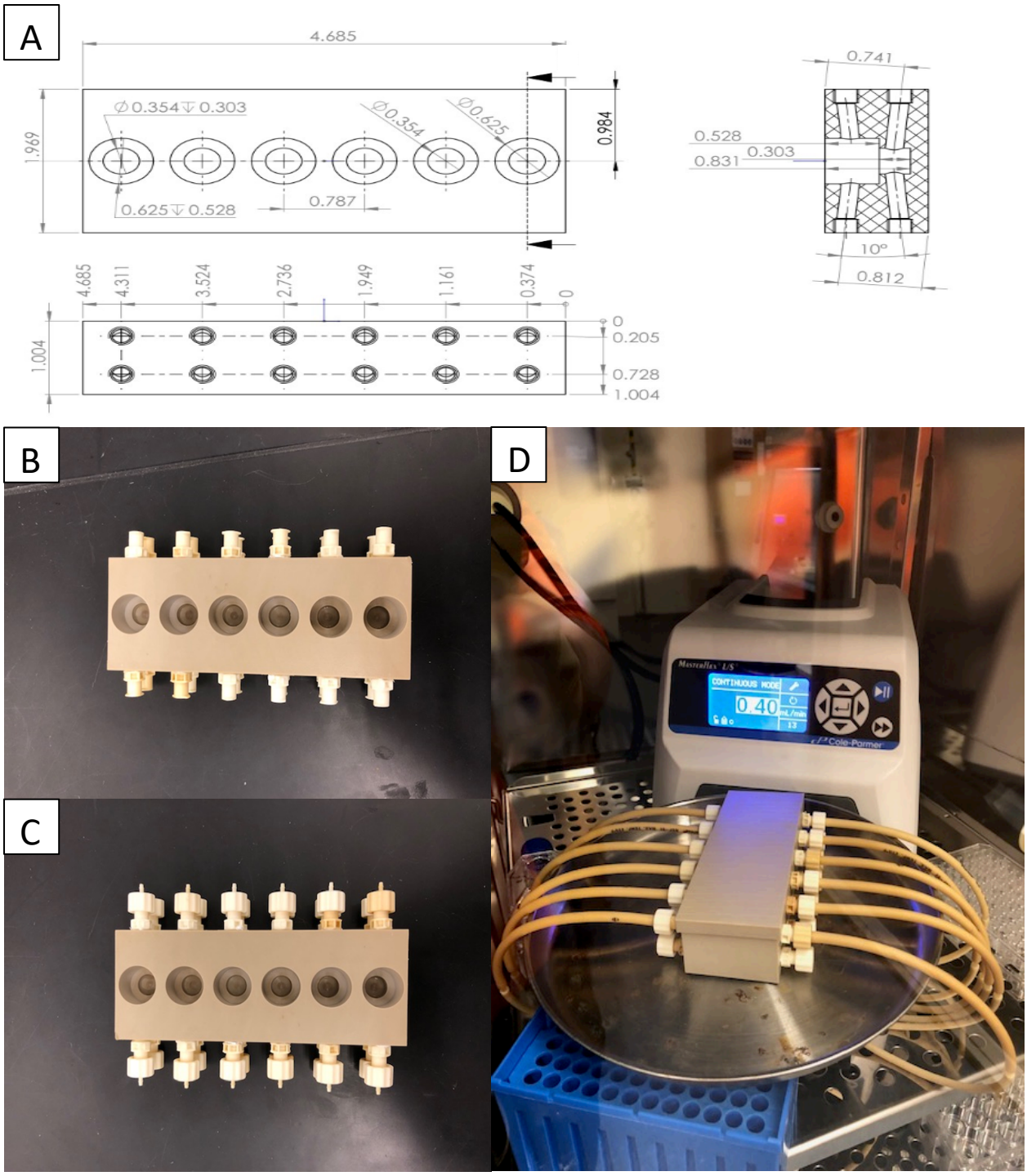

Figure 2. Vascular Bioreactor. (A) Schematic of vascular bioreactor (measurements are in inches). (B) Female luer locks were attached to the bioreactor plate. (C) Male luer locks were connected to the female. For bottom chamber, closed cap pieces were connected. For top chamber, barbed pieces were attached so that tubing could be connected from the pump to the bioreactor. All pieces were then placed in the autoclave to sterilize. (D) Complete bioreactor system set up. After sterilization, connectors were tightened and tubing was connected from the

reactor to the pump. Rings with cells were placed in each well insert followed by the flow rate being set to 0.4 mL/min.

3.2 Design and Fabrication of Rings

Rings were constructed out of the same material as bioreactor and made in-house. To create a surface for cell growth, porous polycarbonate track etch (PCTE) membranes (pore size = 12 μm, 0.52 cm^2; Sterlitech, Kent, WA) were placed in the center of inner rings (ID x OD = 8 x 11.5 mm). This is similar to previous work that used transwells inside of 24-well plates [57]. To secure the membrane, an outer ring (ID x OD = 12 x 15 mm) was snapped around the inner ring (Figure 3A). Rings and membrane were sterilized by autoclave prior to use.

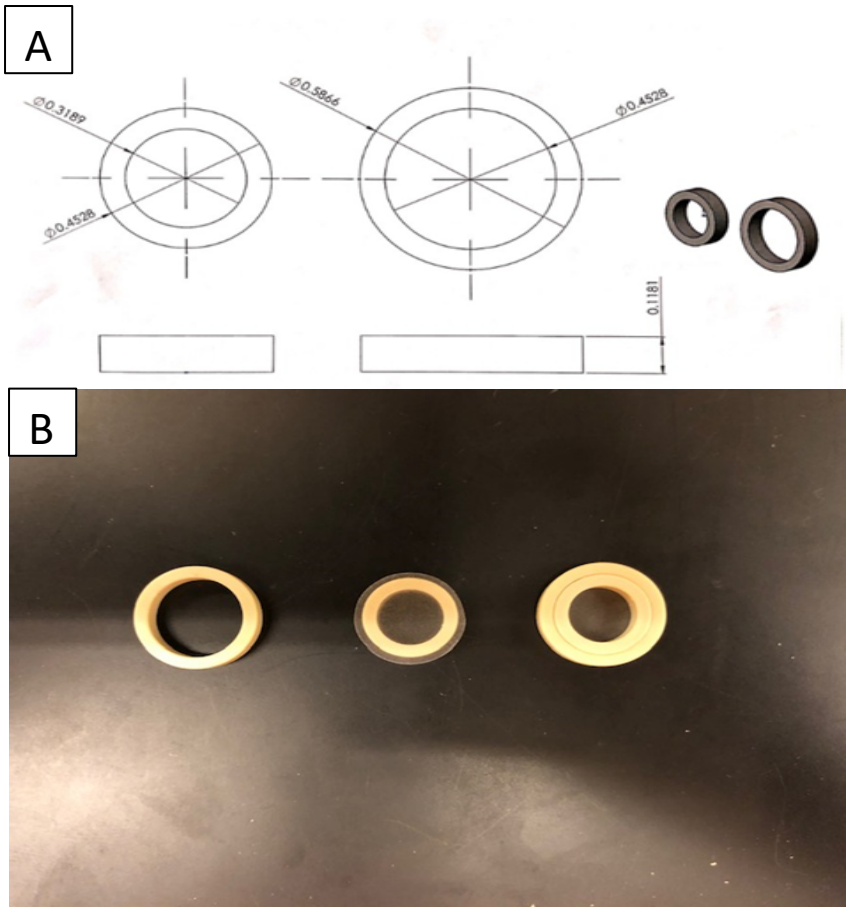

Figure 3. PEEK Rings. (A) Schematic of inner ring (left) and outer ring (right) (measurements are in inches). (B) To create a surface for cells to grow, PCTE membrane was placed over the inner ring. The outer ring was then "snapped" around the inner ring in order to hold the membrane in place.

3.3 Materials

3.3.1 Antibodies and Reagents

Human umbilical vein endothelial cells (HUVECs) and endothelial growth media MV2 were purchased from PromoCell (Heidelberg, Germany). RPMI 1640 (Gibco) media and Penicillin-Streptomycin-Glutamine (PSG) were purchased from ThermoFisher Scientific (Waltham, MA). Human fibronectin was purchased from Alfa Aesar (Tewksbury, MA). Type I bovine collagen

solution was purchased from Advanced BioMatrix (San Diego, CA). Human tumor necrosis factor (TNF-α), rhGM-CSF, rhIL-6, rhIL-4, rhIL-1β and Prostagladin E2 (PGE_2) were purchased from PeproTech (Rocky Hill, NJ). Anti-human fluorochrome-conjugated CD31 (clone WM59), CD54 (clone HCD54), CD106 (clone STA), CD11a/CD18 clone (LFA-1) (clone m24), CD49d (VLA-4) (clone 9F10), HLA-DR (clone L243), CD1c (clone L161), CD206 (MMR, clone 15-2), CD83 (clone HB15e), CD86 (clone BU63), CD3 (clone UCHT1), CD25 (clone BC96) and their respective isotype controls, Ms IgG1 (clone MOPC-21), Ms IgG2a (clone MOPC-173) were purchased from BioLegend (San Diego, CA). Anti-mouse/human CD11b (clone M1/70) and its respective isotype, Ms IgG2b (clone MPC-11) were purchased from BioLegend. Purified anti-human fluorochrome-conjugated CD31 (clone WM59), PE Goat anti-mouse IgG (clone Poly4053) secondary antibody and its isotype, purified Ms IgG1 (clone MOPC-21) were purchased from BioLegend. Tetanus toxoid (TT) was purchased from Sigma-Aldrich (St. Louis, MO). Human MCP-1 ELISA set was purchased from BD Sciences (San Diego, CA). Fetal bovine serum (FBS) was purchased from GE Healthcare Life Sciences (Logan, UT). ProLong Glass Antifade Mountant with NucBlue Stain with DAPI was purchased from Invitrogen (Carlsbad, CA).

3.4 Cell Culture

3.4.1 HUVECs

Membrane rings were coated with a fibronectin (25 μg/mL) and type 1 collagen (3.1 mg/mL) solution for a minimum of 2 h. Media was then added 24 h prior to seeding with cells. HUVECs were cultured in a T-75 flask pretreated with fibronectin for 72 h to reach confluency prior to seeding onto membrane rings. After 72 h, cells were detached with trypsin/EDTA and seeded

onto membrane rings at 100,000 cells/cm^2. Only passages 2-5 were used. ECs were cultured for 72 h in a 24 well cell culture plate (1.9 cm^2, Greiner BioOne, Monroe, NC) to allow for cells to reach confluency on rings. After 72 h, rings were placed in the well inserts in the bioreactor. Using Masterflex L/S pump, flow rate was set to 0.4 mL/min for 72 h. To test for EC response to inflammation, TNF-α (10 ng/mL) was added after 24 h.

3.4.2 Monocytes

Human peripheral blood mononuclear cells (PBMCs) were isolated by the Ficoll-Plague density separation method (GE Healthcare; Pittsburg, PA) from blood of healthy donors obtained from Oklahoma Blood Institute (OBI, Oklahoma City, OK). Autologous plasma was also obtained from OBI. CD14$^+$ monocytes were isolated from PBMCs using CD14 MicroBeads (Miltenyi Biotec, Bergisch Gladbach, Germany). Monocytes were frozen in plasma until use. For migration study, monocytes were stained with carboxyfluorescein succinimidyl ester (CFSE, Invitrogen) prior to addition to bioreactor. Monocyte concentration (500,000 cells/mL) was based on physiological concentration. Monocytes were added to each well after 24 h of culturing HUVECs with or without TNF-α under flow conditions. Monocytes were cultured under 0.4 mL/min flow rate for 48 h based on previous work [5].

3.5 Characterization of HUVECs

3.5.1 Morphology

Morphology of HUVECs on membrane rings was determined by microscopy using Nikon TE2000 fluorescent microscope. Rings were removed from plate bioreactor and placed in a 24-well tissue culture plate. Cells were rinsed with PBS and then fixed with 4% paraformaldehyde. Cells were then blocked with a 5% FBS in PBS solution (v/v) to prevent nonspecific antibonding

binding. Purified CD31 and its respective isotype were prepared in FBS/PBS solution added to each ring to label cellular membrane. PE goat secondary antibody in FBS/PBS was added to increase fluorescent signal. Membranes were then cut out of PEEK rings, placed on glass slides and counterstained with DAPI to label nuclei of HUVECs.

3.5.2 CAM Expression and MCP-1 Release

Expression of CD31 (PECAM-1), CD54 (ICAM-1) and CD106 (VCAM-1) by ECs was determined by flow cytometry using BD Accuri C6 flow cytometer. Trypsinized cells were collected and stained with anti-CD31, anti-CD54 and anti-CD106 or their isotype controls (45 min, 4^{o}C) following manufactures protocol. Viability of cells was determined by use of Zombie Green fixable viability kit (BioLegend). To determine secretion amount of monocyte chemotactic protein (MCP)-1, culture supernatants were collected and stored at -80^{o}C until analysis. Supernatants were analyzed with commercial enzyme-linked immunosorbent assay (ELISA) following manufactures protocol (BD Biosciences, San Diego, CA).

3.6 Characterization of Monocytes

3.6.1 Migration

CFSE stained (0.5 μM) monocytes amounts were calculated based on fluorescent intensity using fluorescent plate reader. CFSE is cell permeant and once inside the cell, the acetate groups are removed by intracellular esterases thus causing the CFSE to strongly bind to amino groups in the cell. Manufactures staining protocol was followed. A standard curve was generated by preparing known monocyte concentrations in media in a 96-well plate in parallel with monocytes in bioreactor. 48 h after monocyte addition, media was collected above and below each ring,

centrifuged and resuspended in media in a 96-well plate. For monocytes located on the endothelial layer, monocytes were detached using trypsin/EDTA, centrifuged and resuspended in media in a 96-well plate. The equation from the standard curve was then used to calculate monocytes at each location.

3.6.2 Surface Marker Expression

Expression of CD11b, CD11a/CD18 (LFA) and CD49d (VLA-4) by monocytes was determined by flow cytometry. Media was collected from above and below the endothelium layer. For monocytes attached to HUVEC layer, trypsin/EDTA was used to lift monocytes off polycarbonate membrane. All samples were centrifuged and stained with anti-CD11b, anti-LFA, and anti-VLA-4 or their isotype controls following manufactures protocol. Marker expression after culture was compared to before at each location and with or without TNF-α.

3.7 Characterization of Monocyte-Derived DCs

3.7.1 Morphology

Morphology of DCs generated in the bioreactor system was determined by microscopy. After 48 h in culture, cells were collected from all locations in bioreactor and resuspended in DPBS. Samples were then stained by Wright-Geisma. Samples were analyzed under light microscopy for DC characteristics of both statically grown and bioreactor generated DCs. DCs were compared to monocytes and between their immature and mature state to observe any morphological changes.

3.7.2 Phenotypic Marker Expression

Expression of HLA-DR, CD1c and CD206 (MMR) was determined by flow cytometry. Collection of was done as stated previously in 3.5.2. All wells were pooled, centrifuged and stained with anti-HLA-DR, anti-CD1c, and anti-CD206 or their isotype controls following manufactures protocol. $CFSE^{+}HLA\text{-}DR^{+}$ cells were analyzed for expression of CD1c and CD206. Number of DCs were identified by expression level of either CD1c, CD206 or both, as these are common DC markers. Those showing negatively for CD1c and CD206 were considered to still be monocytes. Marker expression was compared between location in the bioreactor.

3.7.3 Functionality

MLR was used to determine the functionality of DCs generated in the bioreactor system. Cells were collected from each well in the bioreactor, pooled and distributed between 6 wells in a 96-well round bottom plate in RPMI-1640 containing 250 ng/mL GM-CSF, 100 ng/mL IL-4, 1% PSG, 10% FBS and 30% autologous plasma. DCs were first loaded by adding TT (10 ug/mL) to half of the wells to test DCs ability to take up and process antigens. Loading DCs prior to maturing has shown to promote better interaction and proliferation of T-cells [60]. After 24 h incubation with TT, DCs were pushed toward maturation by adding 10 ng/mL of TNF-α, 10 ng/mL of IL-1β, 1 μg/mL of PGE_2, and 100 U/mL of IL-6 and incubated an additional 24 h prior to MLR. To act as a control, DCs were generated statically by culturing monocytes for 5 days in RPMI-1640 medium containing 1% PSG, 10% FBS, 30% autologous plasma, 250 ng/mL GM-CSF and 100 ng/mL IL-4. Half of media was changed every 48 h. Loading and maturation for static cultured DCs was the same as bioreactor DCs. DCs were analyzed for expression of CD83, CD86 and HLA-DR by flow cytometry after 48 h in bioreactor to determine maturity of cells and

amount of DCs present. DCs were again analyzed after maturation cytokines were added to see if DCs had matured before beginning MLR.

T-cells were isolated from the same donor as monocytes and stored in plasma until use. CD3 Microbeads (Miltenyi Biotec) were used to positively select for T-cells. T-cells were stained with CFSE (1 μM) following manufactures protocol prior to addition with DCs to examine proliferation. DCs and T-cells were mixed at a ratio of 1:10 and incubated for seven days, changing half of the media every other day. Proliferation of T-cells by CFSE decay along with markers CD3 and CD25 were analyzed by flow cytometry after 7 days in culture with DCs. To serve as a control, CFSE labeled and unlabeled T-cells were incubated without DCs in parallel.

3.8 Statistical Analysis

Experimental results are expressed as means ± SD of three samples. For studies using cells isolated from human peripheral blood mononuclear cells, experimental results are expressed as means ± SD of three donors. Student t-test was used for pairwise comparison of groups or between two groups, respectively. A value of $p < 0.05$ was considered significant.

Chapter IV

Results and Discussion

4.1 Characterization of HUVECs

4.1.1 Morphology

The first objective we wanted to ensure was that the bioreactor provided a suitable environment for cells to be cultured in. All wells during each experimental run were cultured in the same manner for with and without TNF-α. Figure 4 shows morphology of HUVECs on the membrane surface. Without TNF-α being added to the system (Figures 4A and 4B), HUVECs showed a tight, compact network and were confluent across the entire membrane. By maintaining this compact network, HUVECs worked to line the PCTE membrane to create a vascular boundary between the upper and lower chamber in the bioreactor. These tight junctions help to regulate what passes through the endothelium, only allowing nutrients or important leukocytes access to area beneath the endothelium. Cells after culture in the bioreactor also appeared wider than those in a static control.

When TNF-α was introduced to the system for 48 h, ECs lost their compact network and became more elongated. ECs also became more spread out and had larger membranes than without TNF-α. Fewer cells appeared on the PCTE membrane which suggest that when TNF-α is added as an inflammatory stimulate, proliferation of ECs decreases [61]. Looser junctions between cell membranes though does allow for more traffic to pass through like macromolecules and cells

[62]. It also allows in conjunction with loose junctions for leukocytes to attach or pass through easier, simulating the beginning of the immune response similar to *in vivo* [63]. This morphological change also is consistent with a previous report where EC aspect ratio increased to around 10 [64].

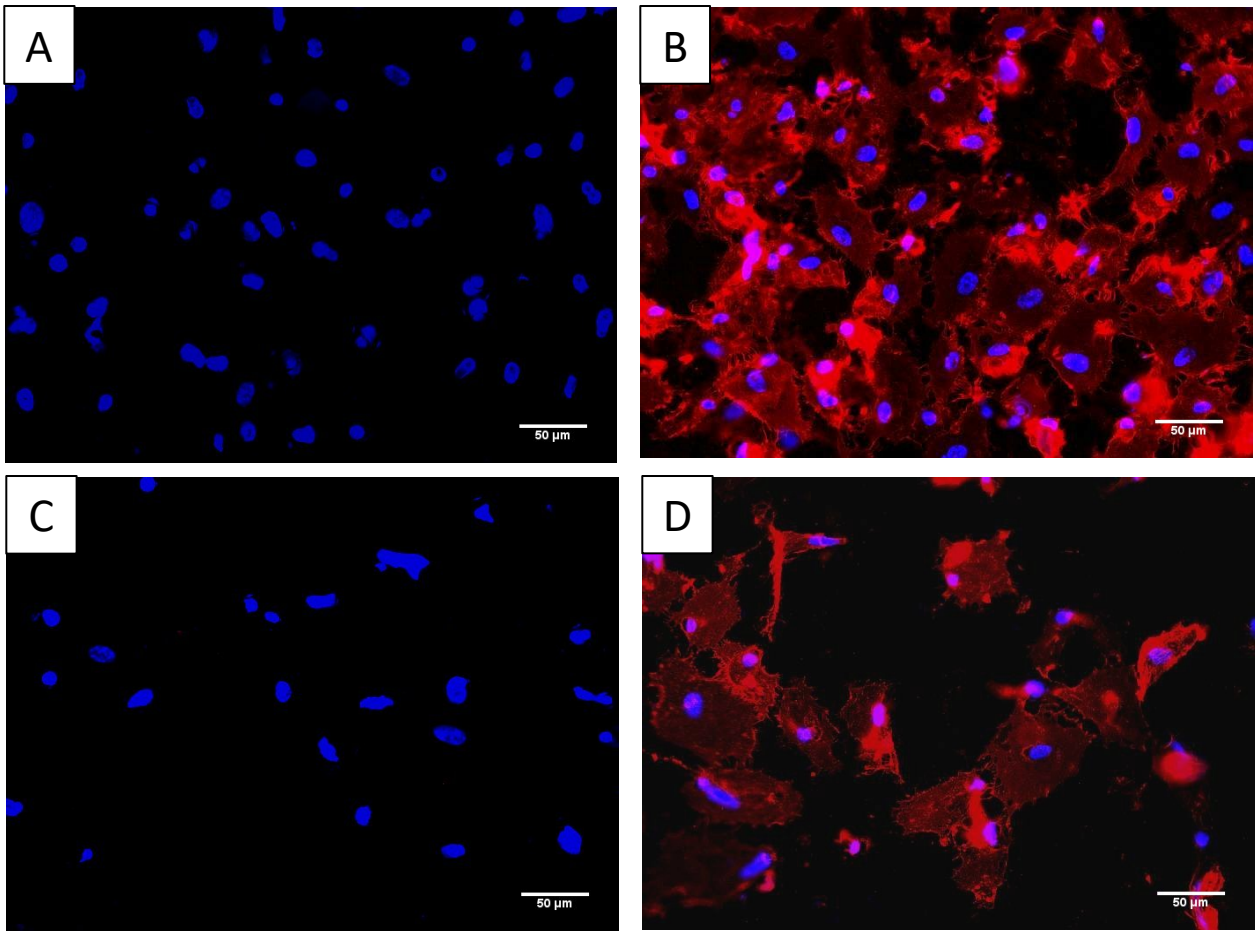

Figure 4. TNF-α treatment changes the morphology of HUVEC's in the plate bioreactor. HUVECs were cultured in the bioreactor for total 72 h. Morphology of HUVECs were examined by staining the cells with anti-PECAM-1 counterstained with DAPI followed by fluorescence microscopy (200x). A and B, cells without TNF-α, C and D, cells with TNF-α added for the final 48 h. A and C, DAPI-stained HUVECs; B and D, HUVECs stained with anti-PECAM antibody counterstained with DAPI. Shown is a representative of the combination of 3 independent experiments.

An interesting result based on morphology is that cells did not align to the direction of flow as others have previously reported [65, 66]. One reason could be due to the system producing disturbed flow, which is where flow is nonuniform and has irregular distribution of low shear stress [67]. This is due to low shear stress and flow path inside our bioreactor can be confirmed by CFD modeling of our system (data not shown). Disturbed flow though is not uncommon in the body and is quite present in veins and arteries at branch points [67, 68]. The results are more closely aligned to previous studies with disturbed flow but did not have any negative on HUVECs effects because of it [62, 68].

4.1.2 CAM Expression and MCP-1 Release

To see HUVEC's response to flow in the bioreactor, we looked at PECAM-1, ICAM-1,VCAM-1 expression along with MCP-1 release. Viability with and without TNF-α were 78% and 82%, respectively. Viable ECs showed high expression (>97%) of ICAM-1 and PECAM-1 after 72 h in bioreactor with and without TNF-α (Figure 5). PECAM-1 is a common marker for ECs and should be expressed on all HUVECs. No alterations in PECAM-1 expression indicates the system does not affect typical HUVEC phenotype. High expression of ICAM-1 has been thought to be due to the change in shear stress the ECs are experiencing compared to if they were statically cultured. ICAM-1 median fluorescent intensity (MFI) increased compared to static ECs (data not shown), indicating cells in the bioreactor are responding similar to previous reports [65, 69, 70]. With TNF-α, ICAM-1 has been shown to influence the contractions ECs are experiencing, causing them to widen and even increase in height [63, 65]. Widening of HUVECS can be seen by the morphological change of HUVECs discussed in 4.1.1.

VCAM-1 is an inflammatory response marker and is upregulated when ECs are stimulated with certain cytokines such as TNF-α [65, 71]. VCAM-1 expression without TNF-α was almost none (5.5%), indicating that HUVECs are not experiencing any sort of inflammatory condition. Shear stress experienced by HUVECs due to flow should also have no effect on the expression of VCAM-1 on ECs [63, 65]. When HUVEC's were activated with TNF-α, VCAM-1 expression on viable ECs was significantly upregulated 37% compared to ECs that were not activated. VCAM-1 plays a role in leukocyte regulation during an inflammatory response. Leukocytes bind to the $\alpha_5\beta_1$ on ECs and VCAM-1 was shown to increase its activation, leading to more cells flowing over the top of the endothelium binding to the EC layer [71]. HUVEC upregulation of VCAM-1 suggests that ECs in bioreactor respond accordingly to inflammatory stimuli.

Similar to VCAM-1, ECs that are stimulated with certain cytokines secrete more MCP-1 than if they were unstimulated. MCP-1 is secreted to recruit monocytes to sites of inflammation [72, 73]. After the addition of TNF-α, concentration of MCP-1 significantly increased 6x than without the inflammatory stimulus (Figure 6). In response to MCP-1, more monocytes infiltrating through the endothelium had been shown in response to increased MCP-1 release by HUVECs [73]. Along with recruitment and migration of monocytes to the endothelium, MCP-1 has been shown to also signal angiogenesis to begin [74, 75]. Unlike a previous study, disturbed flow did not play a role in upregulating MCP-1 [76]. This helps for us to assume that bioreactor itself isn't affecting the HUVECs in a way to behave abnormally even with disturbed flow taking place.

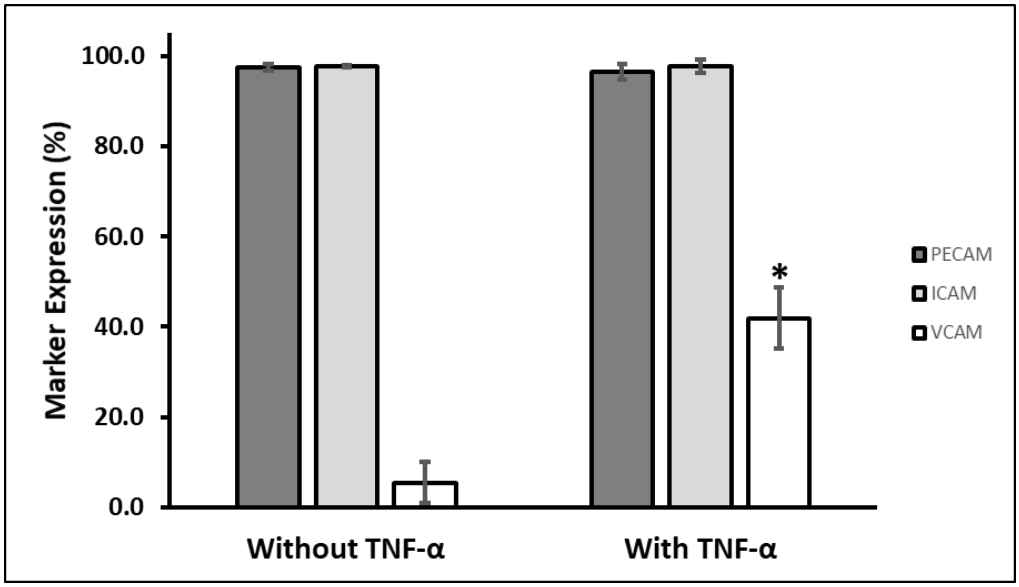

Figure 5. TNF-α selectively alters CAM expression in HUVECs. HUVECs were cultured in the plate bioreactor for total 72 h, and TNF-α was added for the final 48 h. Cells were stained with monoclonal antibodies against CAMs and analyzed by flow cytometry. Data are represented as mean ± SD; n=3. * indicates significantly different ($p < 0.05$) between with and without TNF-α.

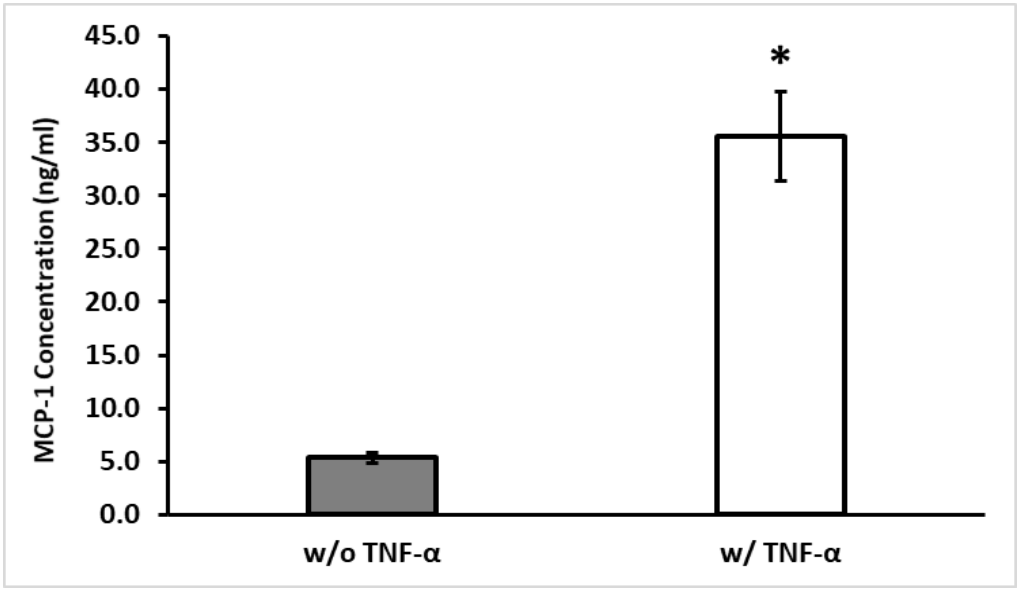

Figure 6. TNF-α significantly increases release of MCP-1 by HUVECs. Media was collected after a total of 72 h for both with and without TNF-α and stored at -80^{o}C until analyzed by ELISA. Data are represented as a mean ± SD; n=3. * indicates significantly different ($p < 0.05$) between with and without TNF-α.

4.2 Characterization of Monocytes

4.2.1 Migration

Monocytes were stained with CFSE to track their location in the bioreactor after being cultured under flow conditions for 48 h. With an unstimulated endothelium, monocytes were relatively the same above and below the endothelium, as shown in Figure 7. Tight junctions created by HUVECs reduced the ability of monocytes to easily pass through the endothelium. Thus, monocytes must first adhere to the endothelium, crawl to a junction and perform diapedesis in order to migrate beneath the HUVEC monolayer. Monocytes beneath the endothelium simulates their infiltration into tissues. When the HUVEC layer was stimulated for 24 h prior to addition of monocytes, monocytes located above the endothelium significantly decreased (49% to 30%), causing more monocytes to migrate through the endothelium (38% to 61%). Without as compact network of HUVECs, monocytes were able to perform diapedesis much easier. The addition of flow as well could have driven more monocytes to migrate through as well [77].

Monocytes attached to the endothelium remained relatively the same regardless of if TNF-α was added to stimulate HUVECs. A small to little change to attachment of monocytes to the endothelium could be due to the limited attachment sites presented by HUVECs. TNF-α stimulated endothelium had been shown to increase monocyte attachment, but that was not the case for monocytes in the bioreactor[78].

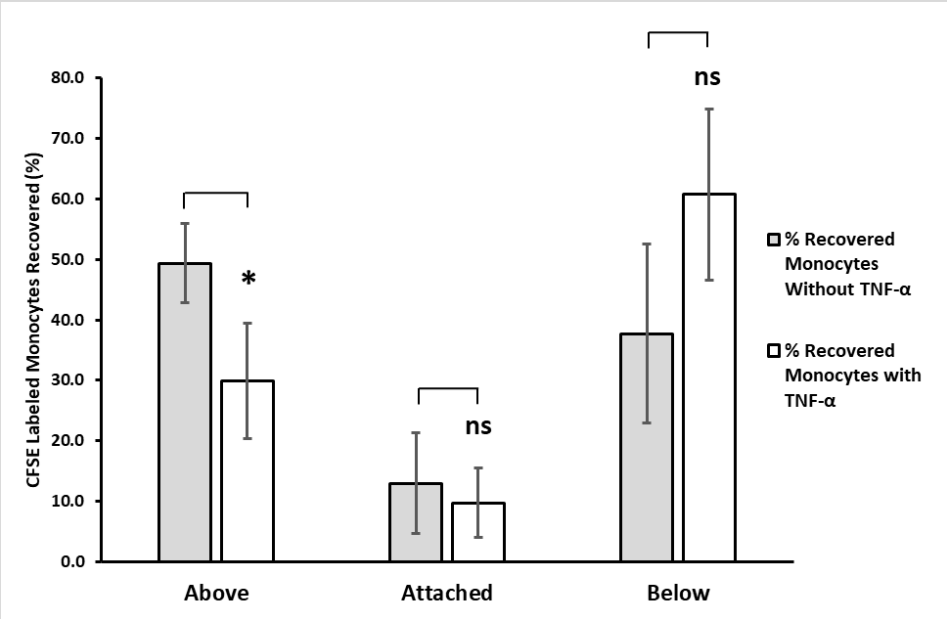

Figure 7. TNF-α affects the localization of monocytes in the plate bioreactor. CFSE-stained monocytes were added to the HUVEC monolayers in the bioreactor and collected after 48 h. Monocytes were lifted from the membranes, as well as collected from the chambers above and below the membranes. Number of monocytes were calculated from a standard curve based on the fluorescent intensities of known monocyte numbers. Data are represented as mean ± SD; n=3. * indicates $p < 0.05$ between with and without TNF-α.

4.2.2 Surface Markers

Monocyte markers CD11b, VLA-4 and LFA were observed as they have been linked to playing a role in monocyte migration [79-81]. Figures 8A-C shows the results of each marker and its expression on monocytes after 48 in culture compared to before addition to bioreactor. Monocytes that were observed were CFSE positive. When the endothelium was not stimulated with TNF-α, CD11b was relatively unchanged in all three locations in the bioreactor. LFA expression increased for monocytes that migrated through the endothelium indicating LFA on monocytes is possibly part of their migration process, which is consistent with a previous report [82]. VLA-4 was downregulated in all locations. Immature DCs have been shown to have low

levels of VLA-4 [83]. The recovered cells not only could be monocytes, but some could be DCs or macrophages.

When HUVECs were stimulated with TNF-α, all phenotypic markers decreased in expression. VLA-4 expression at all locations decreased significantly in expression. This leads us to believe that monocytes are less likely to use VLA-4 during migration in the bioreactor. This is contradictory to previous reports saying VLA-4 is heavily involved in migration of monocytes [84]. Also, decreased expression in VLA-4 could be because cells labeled with CFSE were not monocytes but possibly macrophages or DCs. CD11b expression for monocytes attached to the endothelium and below were significantly downregulated. CD11b has been shown to be downregulated or nonexistent on DCs generated from monocytes [2]. This leads us to believe that when HUVECs are inflamed due to addition of TNF-α, they could be differentiating into DCs [85, 86].

By not labeling for CD16, our system could contain any of the three types of monocytes that have been described earlier. Both CD11b and LFA-1 are part of the β_2 integrin family and have previously been shown to play a role in adhesion and migration of leukocytes. High expression of CD11b indicates that monocytes in the bioreactor are more than likely classical or intermediate monocytes rather than non-classical [87]. CD11b is thought to be involved for firm adhesion of monocytes to endothelium due to its interaction with ICAM-1 [88]. That does not seem to be the case, as CD11b varies only slightly on unstimulated endothelium. For monocytes attached to the activated endothelium, a high downregulation in expression of CD11b could be due to monocytes shifting away from monocyte lineage [89].

LFA-1 has previously been shown to be a factor in migration of monocyte by working with the ICAM-1 ligand on endothelial cells [90]. With little to no decrease in expression of LFA-1, it

may show that adhesion to inflamed tissue by monocytes may actually not use LFA-1 like a previous report suggest [91]. With most previous studies, they looked at migration of monocytes in static systems or for less than 24 h [82, 84]. By adding 24 or more h to the time than previous researchers performed, it could play a role in changing the phenotypes or migration receptors used by monocytes. All this possibly then means that other receptors on monocytes that were not looked at could play a bigger role in migration instead of the ones analyzed in this study for monocytes that are in circulation for a longer period of time.

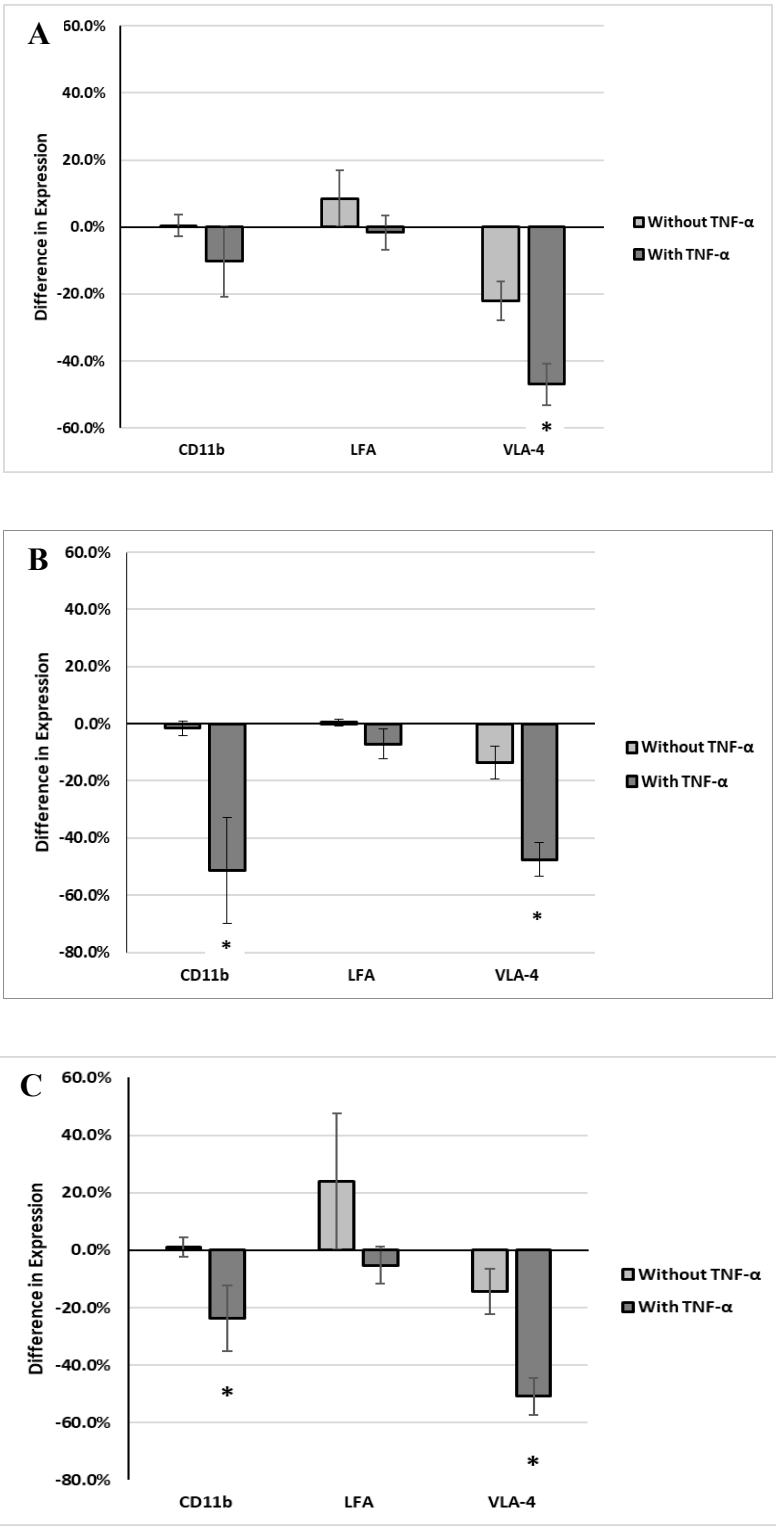

Figure 8. Monocytes downregulate expression of common phenotypic migration markers CD11b and VLA-4 after 48 h under flow conditions with TNF-α. Monocytes were collected at each location and flow cytometry was used to analyze marker expression (A) above (B) attached (C) below endothelium. When compared to with and without TNF-α, VLA-4 expression was

significantly downregulated on monocytes at all locations. LFA-1 expression was slightly upregulated under normal conditions for monocytes that migrated through endothelium. Under inflammatory conditions, expression of CD11b was downregulated at all three locations. Results are represented as difference between before and after culture in bioreactor. Data are represented as mean ± SD; n=3. * indicates significantly different ($p < 0.05$) between with and without TNF-α.

4.3 Characterization of Monocyte-Derived DCs

4.3.1 Morphology

Figure 9 shows morphology of monocyte derived DCs after 48 h in bioreactor (E-H) and statically cultured (A-D). DCs cultured in the bioreactor had no morphological changes compared to those grown in static culture. Nuclei of DCs were rounded, indicating that differentiation had taken place from monocytes as precursor cells have more of a horseshoe shape nuclei. Both also were irregular in cytoplasmic shape, which is typical of DC morphology [92]. This implies that the bioreactor had no ill-effects on DC morphology compared to DCs generated in a 2D static system with cytokines. DCs generated from the bioreactor were almost 2X larger than monocytes. After addition of TT and maturation cytokines, DCs grew dendrites on their surface of the cytoplasm (B, D, F, H), which is a typical indication that maturation has taken place [92]. Further analysis by flow cytometry confirmed that cells were DCs at both immature and mature states. Cytoplasm of mature DCs was also darker in color compared to those in an immature state for bioreactor DCs due to more granules being present.

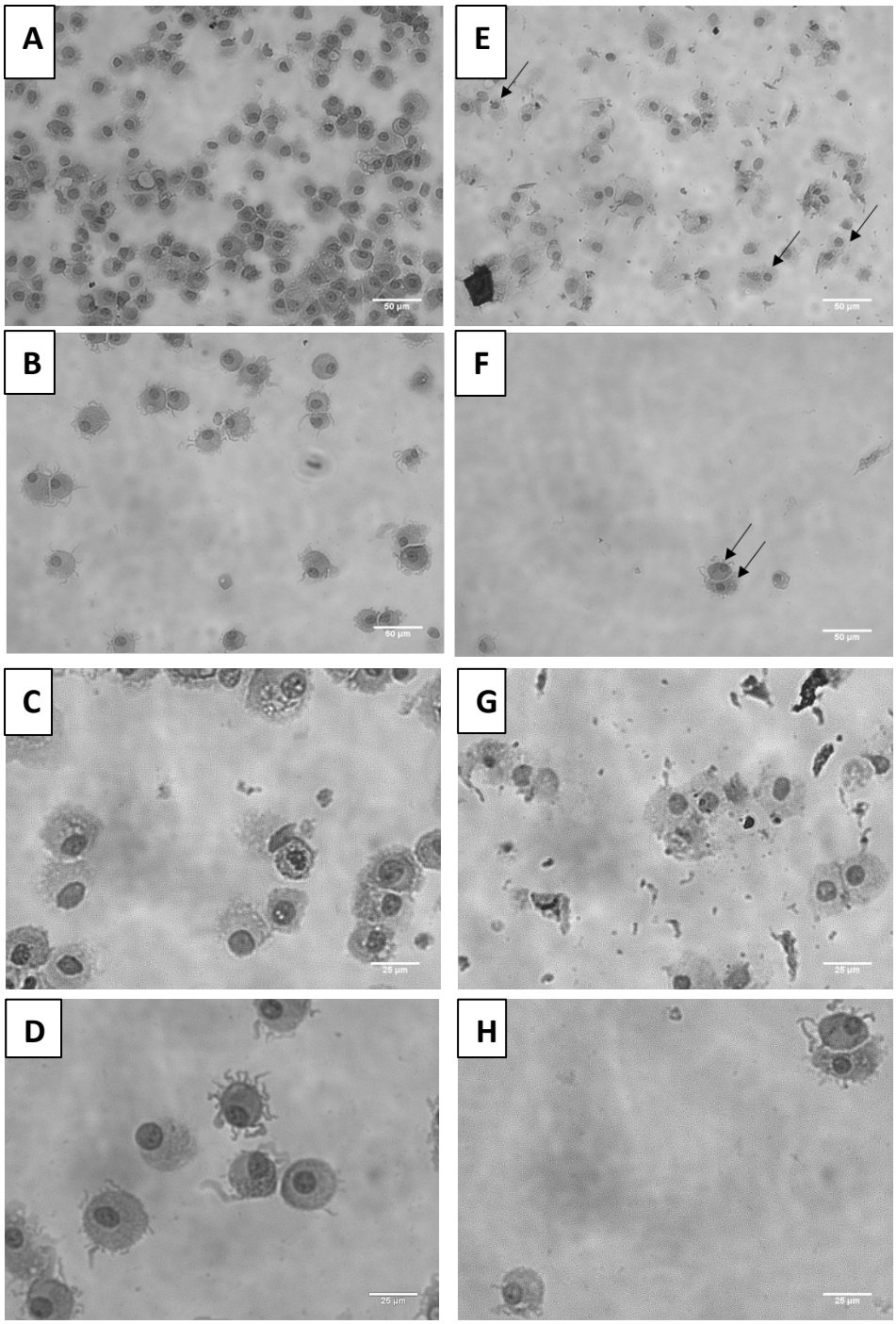

Figure 9. Vascular system has no effect on morphology of monocyte derived DCs. Cells were stained by Wright-Giesma and analyzed with light microscope. (A) & (C) DCs generated in static culture with media containing GM-CSF and IL-4 did not vary in morphology compared to DCs generated after 48 h in vascular bioreactor (E) & (G) After addition of maturation cytokines for 24 h, DCs generated statically (B & D) and bioreactor (F & H) developed dendrites on the surface. Arrows indicate DCs. A, B, E and F were taken at 200X. C, D, G and H were taken at 400X.

4.3.2 Phenotypic Marker Expression

CFSE labeled monocytes were used to gate for differentiated DCs. They were further identified by only looking at HLA-DR$^+$ cells, which is only expressed on antigen presenting cells (APC) and eliminated HUVECs from analysis. If cells were expressing CD1c, CD206 or both, they were considered to be DCs. After 48 h, almost 50% of recovered DCs were located below the endothelium layer (Figure 10). Of those DCs located below the endothelium, there were roughly equal amounts of DCs expressing CD1c and CD206 (Figure 11). One possible reason for more DCs to migrate through could be due to flow, which could drive DCs to migrate rather than remain above or attached. The largest difference in DC population was for DCs attached to the endothelium, where 81% of recovered DCs were expressing CD206 while only 19% expressed CD1c. This could imply that CD206 could play a role in DCs attachment to HUVEC monolayer. Above the endothelium had 37.5% of the DC population and majority of them being CD206$^+$ (62.5%). DCs have been shown to reverse migrate and there is a possibility that CD206 DCs favor reverse migration over CD1c. A high expression was seen on recovered cells for CD14, which is common on monocytes but is typically shed when they differentiate into DCs. When looking at CD14 expression on recovered cells, there were two peaks of expression (data not shown) which indicates that there are two different populations of cells. The peak with a higher fluorescent is presumably still monocytes. The peak that had a lower fluorescent were assumed to be the generated DCs, that had lost the their CD14 expression. Immature DCs had been shown to still express some CD14 to some capacity [34, 35, 93].

Blood monocyte derived DCs do not have one distinct marker to label them. Both CD206 and CD1c had been shown to be present on blood monocyte derived DCs [33, 94, 95]. With different

expression and subsets of DCs, each are unique in their role. CD1c DCs produce more IL-8, which is crucial as a chemoattractant stimulus for other immune response cells [94]. CD1c DCs have also been shown to be the strongest T-cell stimulator when compared to 4 other subsets of DCs from monocytes in MLR experiments [86]. CD206 is important in the antigen uptake performed by DCs [96]. These antigens are later presented to help stimulate T-cell response so they can proliferate and activate other immune response cells.

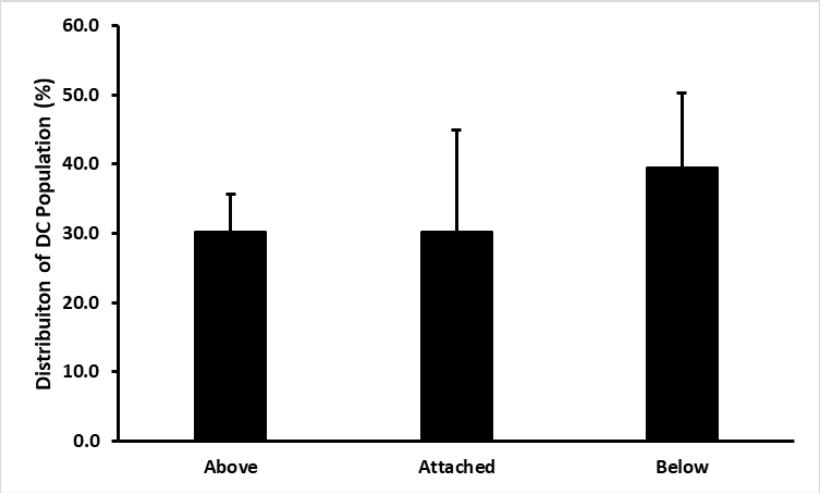

Figure 10. Monocyte derived DCs favor remaining below endothelium after 48 h in bioreactor. Cells were collected from all three locations, stained with anti-CD1c, anti-HLA-DR and anti-CD206 and analyzed by flow cytometry. DCs are $CFSE^{+}HLA\text{-}DR^{+}$ and either CD1c, CD206 or both at that specific location. Data are represented as mean percentage of DC population; n=3.

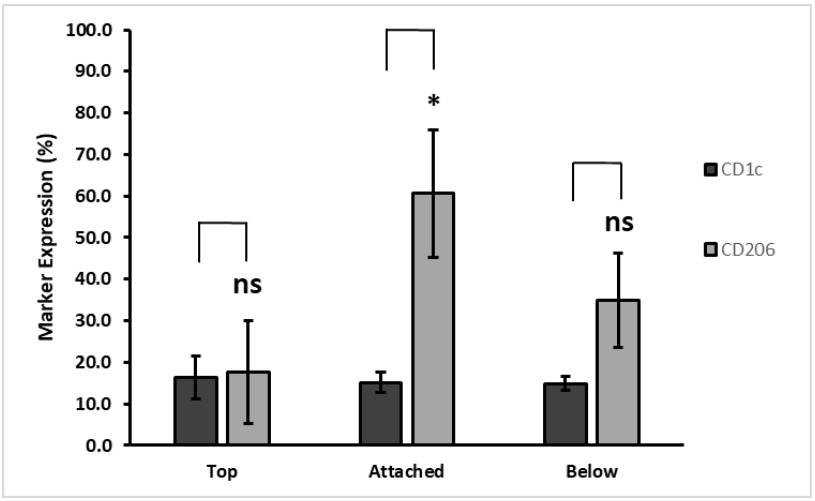

Figure 11. DCs generated in bioreactor system from monocytes expressed more CD206 than CD1c. Cells were collected from all three locations, stained and analyzed for common monocyte derived DC markers. Percentages are of recovered DCs at that specific location. DCs that were above and attached to endothelium had higher expression of CD206 than CD1c. Data are represented as mean percentage; n=3.

4.3.3 Functionality

DCs were collected out of the bioreactor and analyzed first for maturation state. For all analysis, cells were gated for HLA-DR prior to any observation of antibodies. DCs collected out of the bioreactor had a viability of 88.2%, which was comparable to those grown statically (95.9%). Viable bioreactor DCs and statically generated DCs, indicated by their expression of CD86 (89.9 and 88.5%, respectively), both expressed low levels of CD83 before addition of maturation cytokines (Figure 12). After maturation cytokine addition, bioreactor and statically generated DCs significantly upregulated their expression of CD83 (72.0 and 84.9%, respectively). CD86 for both sets had also a higher fluorescent intensity and total amount of cells expressing the marker (>99%) when compared to monocytes and immature DCs, further indicating that maturation of DCs had taken place.

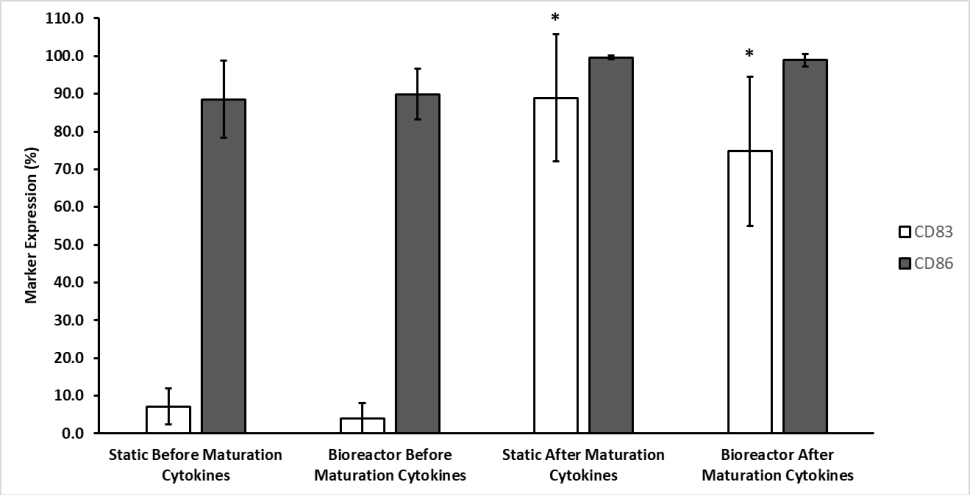

Figure 12. CD83 expression upregulated on DCs after addition of cytokines, an indication of DC maturation. Cells were collected after 2 days in bioreactor or 7 days in static culture. TT was added for 24 h followed by addition of maturation cytokines for 24 h. Results show CD83 and CD86 expression before TT and after addition of maturation cytokines. Data are represented by mean ± SD; n=4. Three separate donors are represented. * indicates significantly different ($p < 0.05$) between before and after maturation cytokine addition.

T-cell proliferation was measured by looking at CFSE decay on $CD3^+CD25^+$ T-cells. CD3 is expressed on all T-cells and is required for antigen recognition [97]. CD25 is upregulated when T-cells have been activated [98]. During proliferation, CFSE is roughly halved every time a cell divides. CFSE has been used quite extensively in T-cell proliferation studies due to its slow release from inside the cell [99]. T-cells analyzed for proliferation were all $CD3^+$ (>99%, data not shown).

Table 1. Expression of CD25 after MLR for 7 days. Data are represented as mean ± SD; n=4. Three separate donors are represented.

	Expression of CD25 (%)
Bioreactor with TT	52.2 ± 25.4
Bioreactor without TT	40.2 ± 19.4
Static with TT	75.4 ± 7.6
Static without TT	60.4 ± 16.5

T-cells with bioreactor DCs had both lower CD25 expression when compared to static cultures under the same conditions. This could possibly be due to DCs dying, thus eliminating a stimulation source. Previous work has shown that T-cells downregulate CD25 after stimulation occurs [100]. T-cells with DCs from the bioreactor loaded with TT expressed roughly 12% more CD25 than T-cells mixed with DCs without any antigen (Table 1).

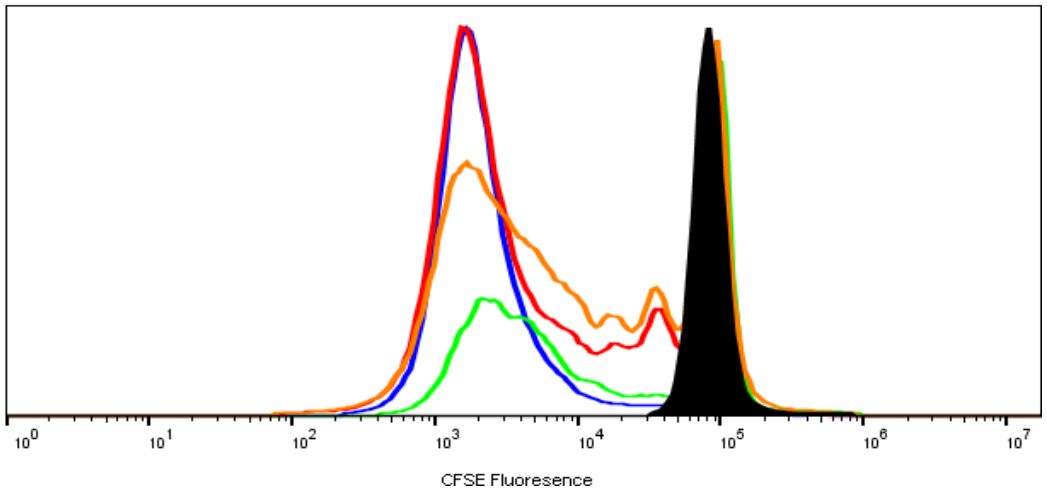

Figure 13. T-cells with DCs preloaded with TT proliferate more than T-cells mixed with unloaded DCs. DCs generated in the bioreactor loaded with TT (blue) induced more proliferation of T-cells than bioreactor DCs without TT (green). The same can be said for DCs from static cultures (with TT = red; without TT = orange). A peak shifted farther left means cells divided since CFSE decay is believed to half every time a cell doubles. Isotype control from Day 0 of T-cells is shown in black. Data are from four experiments; three separate donors are represented.

Even though T-cells had lower expression of CD25 when mixed with bioreactor DCs, bioreactor DCs were able to promote better proliferation of activated T-cells ($CFSE^+CD3^+CD25^+$) than those generated statically. As shown in Figure 13, activated T-cells mixed with DCs loaded with TT were better stimulators for proliferation than those without. Peaks shifted farther to the left indicate more proliferation had occurred since CFSE concentration roughly halves every time a cell divides. Table 2 shows a summary of median fluorescent intensity (MFI) of CFSE of T-cells mixed with DCs. By being able to proliferate more, this in turn promotes an organized and more rapid immune response to stop an infection or disease.

Table 2. Median fluorescent intensity (MFI) of CFSE by activated T-cells after MLR for 7 days. Data are represented as mean ± SD; n=4. Three separate donors are represented.

	CFSE MFI
Bioreactor with TT	2638 ± 2438
Bioreactor without TT	2976 ± 2721
Static with TT	9397 ± 15600
Static without TT	12843 ± 13046

Chapter V

Conclusion

We have developed and characterized a novel bioreactor system that generates functional DCs. The novel bioreactor was able to allow for proper growth and proliferation of ECs on a polycarbonate membrane under flow. Without TNF-α, ECs formed a tight, compact network. When TNF-α was added to simulate inflammation, ECs became elongated and more spread out to possibly allow for more leukocytes to migrate through the endothelium [66]. ECs also significantly increased their VCAM-1 expression and release of MCP-1, both of which have been shown to be common inflammatory responses [71, 72].

To look at migration tendencies of monocytes when added to the bioreactor, monocytes were labeled with CFSE to track location. When endothelium was unstimulated, monocytes above and below the HUVEC monolayer were relatively equal in distribution. When HUVECs were under an inflammatory condition, more monocytes migrated below the endothelium; simulating monocytes entering an inflamed tissue to begin an inflammatory response. This is consistent with Shukla who found that more leukocytes tend to migrate through stimulated endothelium than an unstimulated one [6]. All migration markers on monocytes were downregulated when ECs were pretreated with TNF-α. CD11b's significant downregulation on monocytes when attached or below endothelium could be due to them shifting away from lineage [89]. The significant

downregulation of VLA-4 and CD11b could also be due to monocytes differentiating into DCs where both have been shown to be lost on DCs [2, 83].

DCs in the bioreactor were typical in morphology when compared to statically cultured DCs [92]. A significant increase in CD83 expression on DCs indicates they had matured after the addition of maturation cytokines prior to the MLR [34, 35]. T-cells mixed with DCs from the bioreactor had lower expression of the activation marker CD25. This could be due to DCs dying; thus eliminating T-cell stimulation and starting a downregulation of CD25 expression [100]. DCs with TT had more interaction with T-cells as indicated by the expression of activation marker CD25 on T-cells. For T-cells mixed with bioreactor DCs loaded with TT, DCs had better interaction and stimulation for proliferation of T-cells than without TT. This indicates DCs from the bioreactor are behaving similar to previous studies and have the capability to properly take up, process and present the antigen for T-cells [35, 101]. Activated T-cells proliferated more when mixed with bioreactor DCs than their static counterparts, thus indicating better functionality [102]. Overall, DCs generated in the novel bioreactor were more functional based on ability to stimulate the proliferation of activated T-cells than traditionally generated static DCs.

Chapter VI

Future Work

Optimize the bioreactor by adjusting the height at which cells lie beneath the inlet to create laminar flow over the cells. This could result in better mechanical stimuli for cells to be more viable and have a more typical morphology under flow conditions. Disturbed flow in the bioreactor could be causing a high monocyte death or pushing cells to apoptosis. Eliminating disturbed flow could result in better viability and functionality of DCs that are recovered, resulting in a higher yield of DCs after culture in the bioreactor. Further study into the functionality of the DCs analyzing more surface markers such as CD1a, CD64, CD80 and CCR7 should be done as well. In this study, we did not look into if or how many macrophages were being generated since monocytes can differentiate into either DCs or macrophages. Looking into that could give us a more exact idea on if our system is really favoring DC generation. If not, then further optimizing of the system to favor DCs could be studied.

Studying other designs, such as a tubular form of a bioreactor, to better simulate the vascular network. Initial studies have begun to do so, but creating a vascular scaffold has proven to be quite difficult. This would give a better representation of *in vivo* conditions and could prove to generate more functional DCs than those generated by the plate bioreactor. Using CFD to model it, we can optimize the system to produce the most DCs. At the end, we could compare the plate to tubular reactor to see if it affects the cells any differently.

References

1. Howard, C.J., et al., *The role of dendritic cells in shaping the immune response.* Anim Health Res Rev, 2004. **5**(2): p. 191-5.
2. Banchereau, J. and R.M. Steinman, *Dendritic cells and the control of immunity.* Nature, 1998. **392**(6673): p. 245-52.
3. Steinman, R.M. and M.D. Witmer, *Lymphoid dendritic cells are potent stimulators of the primary mixed leukocyte reaction in mice.* Proc Natl Acad Sci U S A, 1978. **75**(10): p. 5132-6.
4. Sallusto, F. and A. Lanzavecchia, *Efficient presentation of soluble antigen by cultured human dendritic cells is maintained by granulocyte/macrophage colony-stimulating factor plus interleukin 4 and downregulated by tumor necrosis factor alpha.* J Exp Med, 1994. **179**(4): p. 1109-18.
5. Randolph, G.J., et al., *Differentiation of monocytes into dendritic cells in a model of transendothelial trafficking.* Science, 1998. **282**(5388): p. 480-3.
6. Shukla, A., *Effects of Hyperglycemia on Leukocyte Migration and Differentiation in a Novel Three-Dimensional Tissue Model*, in *Graduate College*. 2008, Oklahoma State University: Stillwater, OK. p. 81.
7. Wang, C., et al., *A small diameter elastic blood vessel wall prepared under pulsatile conditions from polyglycolic acid mesh and smooth muscle cells differentiated from adipose-derived stem cells.* Biomaterials, 2010. **31**(4): p. 621-30.
8. Stephenson, M. and W. Grayson, *Recent advances in bioreactors for cell-based therapies.* F1000Res, 2018. **7**.
9. Savary, C.A., et al., *Characteristics of human dendritic cells generated in a microgravity analog culture system.* In Vitro Cell Dev Biol Anim, 2001. **37**(4): p. 216-22.
10. Medzhitov, R., *Inflammation 2010: new adventures of an old flame.* Cell, 2010. **140**(6): p. 771-6.
11. Chen, L., et al., *Inflammatory responses and inflammation-associated diseases in organs.* Oncotarget, 2018. **9**(6): p. 7204-7218.
12. Sugimoto, M.A., et al., *Resolution of Inflammation: What Controls Its Onset?* Front Immunol, 2016. **7**: p. 160.
13. Carmeliet, P. and R.K. Jain, *Molecular mechanisms and clinical applications of angiogenesis.* Nature, 2011. **473**(7347): p. 298-307.
14. Raines, E.W. and N. Ferri, *Thematic review series: The immune system and atherogenesis. Cytokines affecting endothelial and smooth muscle cells in vascular disease.* J Lipid Res, 2005. **46**(6): p. 1081-92.
15. Cines, D.B., et al., *Endothelial cells in physiology and in the pathophysiology of vascular disorders.* Blood, 1998. **91**(10): p. 3527-61.
16. Hauser, S., F. Jung, and J. Pietzsch, *Human Endothelial Cell Models in Biomaterial Research.* Trends in Biotechnology, 2017. **35**(3): p. 265-277.
17. Ley, K. and J. Reutershan, *Leucocyte-endothelial interactions in health and disease.* Handb Exp Pharmacol, 2006(176 Pt 2): p. 97-133.
18. Pober, J.S. and W.C. Sessa, *Evolving functions of endothelial cells in inflammation.* Nat Rev Immunol, 2007. **7**(10): p. 803-15.

19. Stevens, T., et al., *Mechanisms regulating endothelial cell barrier function.* Am J Physiol Lung Cell Mol Physiol, 2000. **279**(3): p. L419-22.
20. Schenkel, A.R., et al., *CD99 plays a major role in the migration of monocytes through endothelial junctions.* Nat Immunol, 2002. **3**(2): p. 143-50.
21. Pober, J.S. and R.S. Cotran, *The role of endothelial cells in inflammation.* Transplantation, 1990. **50**(4): p. 537-44.
22. Shi, C. and E.G. Pamer, *Monocyte recruitment during infection and inflammation.* Nat Rev Immunol, 2011. **11**(11): p. 762-74.
23. Geissmann, F., S. Jung, and D.R. Littman, *Blood monocytes consist of two principal subsets with distinct migratory properties.* Immunity, 2003. **19**(1): p. 71-82.
24. Auffray, C., M.H. Sieweke, and F. Geissmann, *Blood monocytes: development, heterogeneity, and relationship with dendritic cells.* Annu Rev Immunol, 2009. **27**: p. 669-92.
25. Ingersoll, M.A., et al., *Monocyte trafficking in acute and chronic inflammation.* Trends Immunol, 2011. **32**(10): p. 470-7.
26. Yang, J., et al., *Monocyte and macrophage differentiation: circulation inflammatory monocyte as biomarker for inflammatory diseases.* Biomark Res, 2014. **2**(1): p. 1.
27. Kato, M., et al., *Expression of multilectin receptors and comparative FITC-dextran uptake by human dendritic cells.* Int Immunol, 2000. **12**(11): p. 1511-9.
28. Netea, M.G., et al., *Interleukin-32 induces the differentiation of monocytes into macrophage-like cells.* Proc Natl Acad Sci U S A, 2008. **105**(9): p. 3515-20.
29. Liu, K. and M.C. Nussenzweig, *Origin and development of dendritic cells.* Immunol Rev, 2010. **234**(1): p. 45-54.
30. Puhr, S., et al., *Dendritic cell development-History, advances, and open questions.* Semin Immunol, 2015. **27**(6): p. 388-96.
31. Belz, G.T. and S.L. Nutt, *Transcriptional programming of the dendritic cell network.* Nat Rev Immunol, 2012. **12**(2): p. 101-13.
32. Qu, C., et al., *Monocyte-derived dendritic cells: targets as potent antigen-presenting cells for the design of vaccines against infectious diseases.* Int J Infect Dis, 2014. **19**: p. 1-5.
33. Gerlini, G., et al., *Cd1d is expressed on dermal dendritic cells and monocyte-derived dendritic cells.* J Invest Dermatol, 2001. **117**(3): p. 576-82.
34. Gogolak, P., et al., *Differentiation of CD1a- and CD1a+ monocyte-derived dendritic cells is biased by lipid environment and PPARgamma.* Blood, 2007. **109**(2): p. 643-52.
35. Dauer, M., et al., *Mature dendritic cells derived from human monocytes within 48 hours: a novel strategy for dendritic cell differentiation from blood precursors.* J Immunol, 2003. **170**(8): p. 4069-76.
36. Sallusto, F. and A. Lanzavecchia, *The instructive role of dendritic cells on T-cell responses.* Arthritis Res, 2002. **4 Suppl 3**: p. S127-32.
37. Raveney, B.J. and D.J. Morgan, *Dynamic control of self-specific CD8+ T cell responses via a combination of signals mediated by dendritic cells.* J Immunol, 2007. **179**(5): p. 2870-9.
38. Wong, B.R., et al., *TRANCE (tumor necrosis factor [TNF]-related activation-induced cytokine), a new TNF family member predominantly expressed in T cells, is a dendritic cell-specific survival factor.* J Exp Med, 1997. **186**(12): p. 2075-80.
39. Zhou, L.J. and T.F. Tedder, *CD14+ blood monocytes can differentiate into functionally mature CD83+ dendritic cells.* Proc Natl Acad Sci U S A, 1996. **93**(6): p. 2588-92.
40. Witmer-Pack, M.D., et al., *Granulocyte/macrophage colony-stimulating factor is essential for the viability and function of cultured murine epidermal Langerhans cells.* J Exp Med, 1987. **166**(5): p. 1484-98.

41. Castiello, L., et al., *Monocyte-derived DC maturation strategies and related pathways: a transcriptional view.* Cancer Immunol Immunother, 2011. **60**(4): p. 457-66.
42. Lee, A.W., et al., *A clinical grade cocktail of cytokines and PGE2 results in uniform maturation of human monocyte-derived dendritic cells: implications for immunotherapy.* Vaccine, 2002. **20 Suppl 4**: p. A8-A22.
43. Zhao, J., et al., *Bioreactors for tissue engineering: An update.* Biochemical Engineering Journal, 2016. **109**: p. 268-281.
44. Martin, I., D. Wendt, and M. Heberer, *The role of bioreactors in tissue engineering.* Trends Biotechnol, 2004. **22**(2): p. 80-6.
45. Stegemann, J.P. and R.M. Nerem, *Phenotype modulation in vascular tissue engineering using biochemical and mechanical stimulation.* Ann Biomed Eng, 2003. **31**(4): p. 391-402.
46. Barron, V., et al., *Bioreactors for Cardiovascular Cell and Tissue Growth: A Review.* Annals of Biomedical Engineering, 2003. **31**(9): p. 1017-1030.
47. Gary, L.S., et al., *Three-Dimensional Growth of Endothelial Cells in the Microgravity-Based Rotating Wall Vessel Bioreactor.* In Vitro Cellular & Developmental Biology. Animal, 2002. **38**(9): p. 493-504.
48. Dermenoudis, S. and Y. Missirlis, *Design of a novel rotating wall bioreactor for the in vitro simulation of the mechanical environment of the endothelial function.* Journal of Biomechanics, 2010. **43**(7): p. 1426-1431.
49. Rotenberg, M.Y., et al., *A multi-shear perfusion bioreactor for investigating shear stress effects in endothelial cell constructs.* Lab Chip, 2012. **12**(15): p. 2696-703.
50. Punchard, M.A., et al., *Endothelial cell response to biomechanical forces under simulated vascular loading conditions.* J Biomech, 2007. **40**(14): p. 3146-54.
51. Chouinard, J.A., et al., *Design and validation of a pulsatile perfusion bioreactor for 3D high cell density cultures.* Biotechnol Bioeng, 2009. **104**(6): p. 1215-23.
52. Williams, C. and T.M. Wick, *Perfusion bioreactor for small diameter tissue-engineered arteries.* Tissue Eng, 2004. **10**(5-6): p. 930-41.
53. Williams, C. and T.M. Wick, *Endothelial cell-smooth muscle cell co-culture in a perfusion bioreactor system.* Ann Biomed Eng, 2005. **33**(7): p. 920-8.
54. Khismatullin, D.B. and G.A. Truskey, *A 3D numerical study of the effect of channel height on leukocyte deformation and adhesion in parallel-plate flow chambers.* Microvasc Res, 2004. **68**(3): p. 188-202.
55. Luscinskas, F.W., et al., *Monocyte rolling, arrest and spreading on IL-4-activated vascular endothelium under flow is mediated via sequential action of L-selectin, beta 1-integrins, and beta 2-integrins.* J Cell Biol, 1994. **125**(6): p. 1417-27.
56. Chen, C.N., et al., *Neutrophils, lymphocytes, and monocytes exhibit diverse behaviors in transendothelial and subendothelial migrations under coculture with smooth muscle cells in disturbed flow.* Blood, 2006. **107**(5): p. 1933-42.
57. Gappa-Fahlenkamp, H. and A.S. Shukla, *The effect of short-term, high glucose concentration on endothelial cells and leukocytes in a 3D in vitro human vascular tissue model.* In Vitro Cell Dev Biol Anim, 2009. **45**(5-6): p. 234-42.
58. Ma, R. and T. Tang, *Current strategies to improve the bioactivity of PEEK.* Int J Mol Sci, 2014. **15**(4): p. 5426-45.
59. Williams, D., *Polyetheretherketone for long-term implantable devices.* Med Device Technol, 2008. **19**(1): p. 8, 10-1.
60. Schlienger, K., et al., *Efficient priming of protein antigen-specific human CD4(+) T cells by monocyte-derived dendritic cells.* Blood, 2000. **96**(10): p. 3490-8.

61. Luna, C., et al., *TNFalpha-Damaged-HUVECs Microparticles Modify Endothelial Progenitor Cell Functional Activity.* Front Physiol, 2015. **6**: p. 395.
62. Chien, S., *Effects of disturbed flow on endothelial cells.* Ann Biomed Eng, 2008. **36**(4): p. 554-62.
63. Wee, H., et al., *ICAM-1/LFA-1 interaction contributes to the induction of endothelial cell-cell separation: implication for enhanced leukocyte diapedesis.* Exp Mol Med, 2009. **41**(5): p. 341-8.
64. Stroka, K.M., J.A. Vaitkus, and H. Aranda-Espinoza, *Endothelial cells undergo morphological, biomechanical, and dynamic changes in response to tumor necrosis factor-alpha.* Eur Biophys J, 2012. **41**(11): p. 939-47.
65. Nagel, T., et al., *Shear stress selectively upregulates intercellular adhesion molecule-1 expression in cultured human vascular endothelial cells.* J Clin Invest, 1994. **94**(2): p. 885-91.
66. Seebach, J., et al., *Regulation of endothelial barrier function during flow-induced conversion to an arterial phenotype.* Cardiovasc Res, 2007. **75**(3): p. 596-607.
67. Chiu, J.J. and S. Chien, *Effects of disturbed flow on vascular endothelium: pathophysiological basis and clinical perspectives.* Physiol Rev, 2011. **91**(1): p. 327-87.
68. Miao, H., et al., *Effects of flow patterns on the localization and expression of VE-cadherin at vascular endothelial cell junctions: in vivo and in vitro investigations.* J Vasc Res, 2005. **42**(1): p. 77-89.
69. Tsuboi, H., et al., *Flow stimulates ICAM-1 expression time and shear stress dependently in cultured human endothelial cells.* Biochem Biophys Res Commun, 1995. **206**(3): p. 988-96.
70. Relou, I.A., et al., *Effect of culture conditions on endothelial cell growth and responsiveness.* Tissue Cell, 1998. **30**(5): p. 525-30.
71. Sun, W.Y., S.M. Pitson, and C.S. Bonder, *Tumor necrosis factor-induced neutrophil adhesion occurs via sphingosine kinase-1-dependent activation of endothelial {alpha}5{beta}1 integrin.* Am J Pathol, 2010. **177**(1): p. 436-46.
72. Rollins, B.J., et al., *Cytokine-activated human endothelial cells synthesize and secrete a monocyte chemoattractant, MCP-1/JE.* Am J Pathol, 1990. **136**(6): p. 1229-33.
73. Carr, M.W., et al., *Monocyte chemoattractant protein 1 acts as a T-lymphocyte chemoattractant.* Proc Natl Acad Sci U S A, 1994. **91**(9): p. 3652-6.
74. Salcedo, R., et al., *Human endothelial cells express CCR2 and respond to MCP-1: direct role of MCP-1 in angiogenesis and tumor progression.* Blood, 2000. **96**(1): p. 34-40.
75. Schratzberger, P., et al., *Release of chemoattractants for human monocytes from endothelial cells by interaction with neutrophils.* Cardiovasc Res, 1998. **38**(2): p. 516-21.
76. Balaguru, U.M., et al., *Disturbed flow mediated modulation of shear forces on endothelial plane: A proposed model for studying endothelium around atherosclerotic plaques.* Sci Rep, 2016. **6**: p. 27304.
77. Cinamon, G., V. Shinder, and R. Alon, *Shear forces promote lymphocyte migration across vascular endothelium bearing apical chemokines.* Nat Immunol, 2001. **2**(6): p. 515-22.
78. Maus, U., et al., *Role of endothelial MCP-1 in monocyte adhesion to inflamed human endothelium under physiological flow.* Am J Physiol Heart Circ Physiol, 2002. **283**(6): p. H2584-91.
79. Shang, X.Z. and A.C. Issekutz, *Contribution of CD11a/CD18, CD11b/CD18, ICAM-1 (CD54) and -2 (CD102) to human monocyte migration through endothelium and connective tissue fibroblast barriers.* Eur J Immunol, 1998. **28**(6): p. 1970-9.
80. Gerhardt, T. and K. Ley, *Monocyte trafficking across the vessel wall.* Cardiovasc Res, 2015. **107**(3): p. 321-30.
81. Kukreti, S., et al., *Molecular mechanisms of monocyte adhesion to interleukin-1beta-stimulated endothelial cells under physiologic flow conditions.* Blood, 1997. **89**(11): p. 4104-11.

82. Meerschaert, J. and M.B. Furie, *The adhesion molecules used by monocytes for migration across endothelium include CD11a/CD18, CD11b/CD18, and VLA-4 on monocytes and ICAM-1, VCAM-1, and other ligands on endothelium.* J Immunol, 1995. **154**(8): p. 4099-112.
83. Puig-Kroger, A., et al., *Maturation-dependent expression and function of the CD49d integrin on monocyte-derived human dendritic cells.* J Immunol, 2000. **165**(8): p. 4338-45.
84. Chuluyan, H.E. and A.C. Issekutz, *VLA-4 integrin can mediate CD11/CD18-independent transendothelial migration of human monocytes.* J Clin Invest, 1993. **92**(6): p. 2768-77.
85. Thomas, R. and P.E. Lipsky, *Human peripheral blood dendritic cell subsets. Isolation and characterization of precursor and mature antigen-presenting cells.* J Immunol, 1994. **153**(9): p. 4016-28.
86. MacDonald, K.P., et al., *Characterization of human blood dendritic cell subsets.* Blood, 2002. **100**(13): p. 4512-20.
87. Boyette, L.B., et al., *Phenotype, function, and differentiation potential of human monocyte subsets.* PLoS One, 2017. **12**(4): p. e0176460.
88. Diamond, M.S., et al., *ICAM-1 (CD54): a counter-receptor for Mac-1 (CD11b/CD18).* J Cell Biol, 1990. **111**(6 Pt 2): p. 3129-39.
89. Tso, C., K.A. Rye, and P. Barter, *Phenotypic and functional changes in blood monocytes following adherence to endothelium.* PLoS One, 2012. **7**(5): p. e37091.
90. Marlin, S.D. and T.A. Springer, *Purified intercellular adhesion molecule-1 (ICAM-1) is a ligand for lymphocyte function-associated antigen 1 (LFA-1).* Cell, 1987. **51**(5): p. 813-9.
91. Meisel, S.R., et al., *Increased expression of neutrophil and monocyte adhesion molecules LFA-1 and Mac-1 and their ligand ICAM-1 and VLA-4 throughout the acute phase of myocardial infarction: possible implications for leukocyte aggregation and microvascular plugging.* J Am Coll Cardiol, 1998. **31**(1): p. 120-5.
92. Tan, Y.F., C.F. Leong, and S.K. Cheong, *Observation of dendritic cell morphology under light, phase-contrast or confocal laser scanning microscopy.* Malays J Pathol, 2010. **32**(2): p. 97-102.
93. Chapuis, F., et al., *Differentiation of human dendritic cells from monocytes in vitro.* Eur J Immunol, 1997. **27**(2): p. 431-41.
94. Lundberg, K., et al., *Human blood dendritic cell subsets exhibit discriminative pattern recognition receptor profiles.* Immunology, 2014. **142**(2): p. 279-88.
95. Jakobsen, M.A., B.K. Moller, and S.T. Lillevang, *Serum concentration of the growth medium markedly affects monocyte-derived dendritic cells' phenotype, cytokine production profile and capacities to stimulate in MLR.* Scand J Immunol, 2004. **60**(6): p. 584-91.
96. Stahl, P.D. and R.A. Ezekowitz, *The mannose receptor is a pattern recognition receptor involved in host defense.* Curr Opin Immunol, 1998. **10**(1): p. 50-5.
97. Heath, W.R., *T Lymphocytes*, in *Encyclopedia of Immunology (Second Edition)*, P.J. Delves, Editor. 1998, Elsevier: Oxford. p. 2341-2343.
98. Cantrell, D., *Signaling in lymphocyte activation.* Cold Spring Harb Perspect Biol, 2015. **7**(6).
99. Rubio, M.T., et al., *Maturation of human monocyte-derived dendritic cells (MoDCs) in the presence of prostaglandin E2 optimizes CD4 and CD8 T cell-mediated responses to protein antigens: role of PGE2 in chemokine and cytokine expression by MoDCs.* Int Immunol, 2005. **17**(12): p. 1561-72.
100. Hedfors, I.A. and J.E. Brinchmann, *Long-term proliferation and survival of in vitro-activated T cells is dependent on Interleukin-2 receptor signalling but not on the high-affinity IL-2R.* Scand J Immunol, 2003. **58**(5): p. 522-32.
101. Osugi, Y., S. Vuckovic, and D.N. Hart, *Myeloid blood CD11c(+) dendritic cells and monocyte-derived dendritic cells differ in their ability to stimulate T lymphocytes.* Blood, 2002. **100**(8): p. 2858-66.

102. Parish, C.R., *Fluorescent dyes for lymphocyte migration and proliferation studies.* Immunol Cell Biol, 1999. **77**(6): p. 499-508.

Appendix

Appendix A: Tubular Reactor

A tubular bioreactor was created but was not tested during this project. Figures A1 shows the bioreactor. The material of for the reactor chamber is the same as that for the plate bioreactor. Different variations to create a tubular mold had been tried but were unsuccessful. Right now, developing a sterilization technique for a collagen/chitosan solution would be the best method. A stainless steel mold has been fabricated. After adding collagen/chitosan solution into the mold, it is frozen at 4^{o}C for 2 h. After 2 h, the center rod is removed and lyophilized for 24 h. After 24, the scaffold is removed from the outer mold and the rod is reinserted into the annular of the scaffold to maintain inner diameter which is then placed a 1% TPP solution for 24 to crosslink. After 24 h, the scaffold is washed 5X with Ultrapure water and refrozen at 4^{o}C for 2 h. It is again placed back on the freeze dryer to be lyophilized for 24 h.

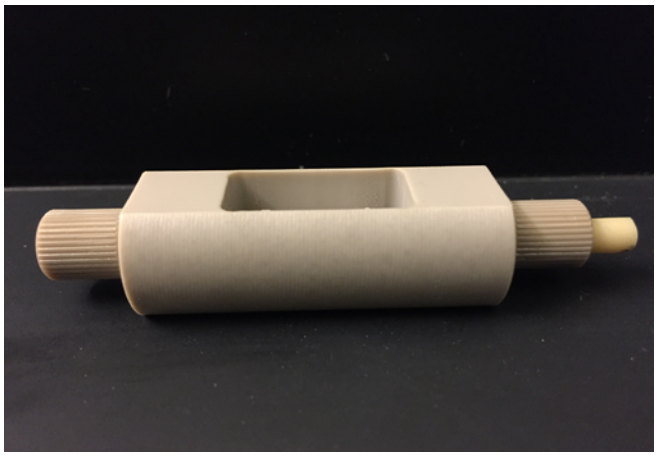

Figure 1A. Tubular bioreactor.

The tubular scaffold then needs to be scaffold and attempts to do have been done. By placing it in a 70% ethanol solution for 24 h followed by UV sterilization has seen some success but does not work every time.

VITA

Patrick Stephen Williamson

Candidate for the Degree of

Master of Science

Thesis: INTERACTION OF MONOCYTES AND ENDOTHELIAL CELLS WITHIN A VASCULAR BIOREACTOR

Major Field: Chemical Engineering

Biographical:

Education:

Completed the requirements for the Master of Science in Chemical Engineering at Oklahoma State University, Stillwater, Oklahoma in August, 2019.

Completed the requirements for the Bachelor of Science in Chemical Engineering at Oklahoma State University, Stillwater, Oklahoma in May, 2017.

Experience:

Graduate Teaching Assistant, College of Engineering, Architecture and Technology, Oklahoma State University Aug. 2017-May 2019

Professional Memberships:

American Institute of Chemical Engineers (AIChE)